



# Characterization of purinergic signaling in tumor-infiltrating lymphocytes from lower- and high-grade gliomas

Juliete Nathali Scholl<sup>1</sup> · Augusto Ferreira Weber<sup>1</sup> · Camila Kehl Dias<sup>1</sup> · Vinícius Pierdoná Lima<sup>1</sup> · Lucas Kich Grun<sup>2</sup> · Diego Zambonin<sup>3</sup> · Eduardo Anzolin<sup>3</sup> · Wanderson Willian Dos Santos Dias<sup>3</sup> · Willian Pegoraro Kus<sup>3</sup> · Florencia Barbé-Tuana<sup>4</sup> · Ana Maria Oliveira Battastini<sup>1</sup> · Paulo Valdeci Worm<sup>3,5</sup> · Fabrício Figueiró<sup>1,6</sup>

Received: 8 December 2022 / Accepted: 6 March 2023  
© The Author(s), under exclusive licence to Springer Nature B.V. 2023

## Abstract

Malignant gliomas are highly heterogeneous glia-derived tumors that present an aggressive and invasive nature, with a dismal prognosis. The multi-dimensional interactions between glioma cells and other tumor microenvironment (TME) non-tumoral components constitute a challenge to finding successful treatment strategies. Several molecules, such as extracellular purines, participate in signaling events and support the immunosuppressive TME of glioma patients. The purinergic signaling and the ectoenzymes network involved in the metabolism of these extracellular nucleotides are still unexplored in the glioma TME, especially in lower-grade gliomas (LGG). Also, differences between IDH-mutant (IDH-Mut) versus wild-type (IDH-WT) gliomas are still unknown in this context. For the first time, to our knowledge, this study characterizes the TME of LGG, high-grade gliomas (HGG) IDH-Mut, and HGG IDH-WT patients regarding purinergic ectoenzymes and P1 receptors, focusing on tumor-infiltrating lymphocytes. Here, we show that ectoenzymes from both canonical and non-canonical pathways are increased in the TME when compared to the peripheral blood. We hypothesize this enhancement supports extracellular adenosine generation, hence increasing TME immunosuppression.

**Keywords** Glioma · Tumor Microenvironment · Purinergic Signaling · Adenosine

**Juliete Nathali Scholl** Graduated in Biomedical Sciences at the Federal University of Health Sciences of Porto Alegre. She is currently a Ph.D. candidate at the Federal University of Rio Grande do Sul, focusing on the characterization of different components of the tumor microenvironment of glioma patients, in particular on the role of purinergic signaling and extracellular vesicles in immunomodulation and tumor progression.



✉ Fabrício Figueiró  
fabricio.figueiro@ufrgs.br

<sup>1</sup> Programa de Pós-Graduação Em Ciências Biológicas: Bioquímica, Instituto de Ciências Básicas da Saúde, UFRGS, Porto Alegre, RS, Brazil

<sup>2</sup> Programa de Pós-Graduação Em Pediatria E Saúde da Criança, Escola de Medicina, PUCRS, Porto Alegre, RS, Brazil

<sup>3</sup> Departamento de Neurocirurgia, Hospital Cristo Redentor, Porto Alegre, Brazil

<sup>4</sup> Programa de Pós-Graduação Em Biologia Celular E Molecular, Escola de Ciências da Saúde E da Vida, PUCRS, Porto Alegre, RS, Brazil

<sup>5</sup> Departamento de Cirurgia, Universidade Federal de Ciências da Saúde de Porto Alegre, Rio Grande Do Sul, Porto Alegre, Brazil

<sup>6</sup> Departamento de Bioquímica, Instituto de Ciências Básicas da Saúde, UFRGS, Porto Alegre, RS, Brazil

## Introduction

Diffuse gliomas are the most prevalent and aggressive malignant Central Nervous System (CNS) tumors. Lower-grade gliomas (LGG, World Health Organization [WHO] grade II and III) exhibit an invasive nature and a high risk to progress or recur to high-grade gliomas (HGG, WHO grade IV) [1]. Grade IV astrocytoma, or glioblastoma (GB), represents the most aggressive subtype, with a consistently dismal prognosis of less than 15 months [2]. In contrast, LGGs are less aggressive. To date, molecular features, such as isocitrate dehydrogenase (IDH) mutation, correlate with the prognosis of malignant glioma more closely than histological criteria alone [3].

IDH is a metabolic enzyme that catalyzes the oxidative decarboxylation of isocitrate to  $\alpha$ -ketoglutarate. Cancer-associated IDH mutation is a driver mutation of malignant gliomas and a variety of other cancers [4], such as acute myeloid leukemia [5], colorectal cancer [6], chondrosarcoma [7], prostate cancer [8], and melanoma [9]. The mutant IDH enzyme catalyzes the conversion of  $\alpha$ -ketoglutarate to 2-hydroxyglutarate (2HG), an oncometabolite [10] capable of blocking cell differentiation and promoting self-renewal of stem-like progenitor cells, which can create a permissive microenvironment for malignant transformation [11]. Nonetheless, IDH1/2-mutant (Mut) gliomas were associated with a better outcome than IDH1/2 wild-type (WT) tumors. It remains unclear what drives this patient survival advantage; however, literature shows IDH-Mut tumors exhibit a favorable response to radio- and chemotherapy [12] and a distinct tumor immune microenvironment [13].

The interaction between non-tumoral and tumor cells can lead to tumor growth, influencing patient outcome. The non-malignant TME is composed of neuronal precursor cells, endothelial cells, fibroblasts, and immune cells, such as macrophages/microglia, dendritic cells, natural killer (NK) cells, and lymphocytes [14]. The immune TME portrays a dual role in glioma: whilst immune cells exert influence to support control of glioma, tumor cells shape this immune infiltrate to promote immune suppression and evasion [15]. Tumor-infiltrating lymphocytes (TILs) comprise the adaptive immunity, generally outnumbered by cells from innate immunity such as tumor-associated macrophages (TAM) in the TME [16]. The lymphocytic infiltrate includes CD4<sup>+</sup> T helper (Th) cells, CD8<sup>+</sup> cytotoxic T lymphocytes (CTLs), CD4<sup>+</sup> regulatory T cells (Tregs; CD4<sup>+</sup>CD25<sup>high</sup>FoxP3<sup>+</sup>), and B cells. The antitumor effects are mainly mediated by Th and CTLs through the secretion of proinflammatory cytokines, such as IFN- $\gamma$ , TNF- $\alpha$ , and IL-2, and cytotoxic granules containing perforin and granzyme, respectively [17]. Further, NK cells (CD3<sup>-</sup>CD56<sup>+</sup>) are cytotoxic innate lymphoid cells that are the first line of defense to attack and eliminate

cancer cells [18]. Conversely, Treg cells produce a powerful immunosuppressor effect, impairing T effector (Teff) and NK cells proliferation through contact-dependent mechanisms or cytokine secretion, such as TFG- $\beta$  and IL-10 [18]. Similarly, B lymphocytes can either suppress (suppressive B cells — CD19<sup>+</sup>CD39<sup>high</sup>) or stimulate the immune system's effector response, generating an anti- or pro-tumor response, depending on the signal received [19].

In the TME, Tregs and Bregs overexpress the enzyme NTPDase1/CD39 [19, 20], and, in coordination with glioma cells, that overexpress ecto-5'-nucleotidase/CD73 [21], produce adenosine (ADO) by sequential extracellular hydrolysis of ATP. Recently, an alternative, non-canonical pathway for ADO formation has been proposed, involving CD38 hydrolysis of NAD<sup>+</sup>, producing adenosine diphosphate ribose (ADPR) or cyclic ADPR (cADPR), which is hydrolyzed by the ectopyrophosphatase/phosphodiesterase1 (NPP1/CD203a), promoting AMP formation. CD203a can also hydrolyze NAD<sup>+</sup> directly, generating AMP. Both mechanisms end in CD73, generating immunosuppressive ADO [22]. Extracellular ADO, in turn, can suppress the proliferation of Teff and NK cells, thus promoting a protumor environment. This ADO acts on specific plasma membrane G-protein coupled receptors (P1 receptors; A<sub>1</sub>, A<sub>2A</sub>, A<sub>2B</sub>, and A<sub>3</sub>), promoting tumor cell invasion, proliferation, and survival [23]. Also, A<sub>2A</sub> is the main P1 receptor found in lymphocytes. When stimulated, it inhibits pro-inflammatory cytokines production and effector functions in T cells; activating, on the other hand, Treg cells [24]

Until now, extensive data has been published about GB TME. However, little is known about purinergic enzymes and receptors in LGG. Also, the literature lacks a purinergic characterization of tumor immunologic profile, especially one that stratifies patients according to tumor grade (LGG and HGG). Here, we present a comprehensive purinergic characterization of the TME of glioma patients, comparing LGG and HGG tumors, focusing on both immune and tumor cells. Furthermore, we explore how IDH mutations can influence the immunological microenvironment of HGG associated with purinergic signaling.

## Materials and methods

### Chemicals

Dulbecco's Modified Eagle Medium: Nutrient Mixture F-12 (DMEM/F-12), Fetal Bovine Serum (FBS), Fungizone®, penicillin/streptomycin, and 0.5% trypsin/EDTA solution were obtained from Gibco (Gibco BRL, CA, USA). Collagenase IV, Dimethyl sulfoxide (DMSO), adenosine-5'triphosphate (ATP), adenosine-5'diphosphate (ADP), adenosine-5'monophosphate (AMP), adenosine (ADO),

**Table 1** Characteristics of the analyzed cohort

	Lower-Grade Glioma	High-Grade Glioma IDH Mutant	High-Grade Glioma IDH Wild-type
Case, n (%)	7 (25%)	9 (32%)	12 (43%)
Male sex – n° (%)	4 (14.2%)	5 (17.8%)	10 (35.7%)
WHO grade, n (%)			
Grade II	5 (17.8%)		
Grade III	2 (7.1%)		
Grade IV		9 (32%)	12 (43%)
Age at diagnosis			
Median	36	63,5	59
Range	24–59	47–84	16–72

inosine (INO), hypoxanthine (HYPOX), xanthine (XANT), uric acid (UA), Coomassie brilliant blue G, Tris–HCl, methanol, tetrabutylammonium hydroxide, and potassium phosphate monobasic were obtained from Sigma Aldrich (USA). DNase (Ambion, USA). All other chemicals and solvents used were of analytical or pharmaceutical grade.

### Sample processing

Fresh surgically resected astrocytoma tissues and peripheral blood samples were collected at the Hospital Cristo Redentor, after informed patient consent, between January 2021 and June 2022. A total of 28 patient cases from both female and male subjects between the ages of 16–84 years were included in the present study. The epidemiological and histological data for each sample are detailed in Table 1 and supplementary Table 1. Astrocytoma grades II, III, and IV were confirmed by pathological assessment of the resected tumors, which were classified according to the WHO Classification of Tumors of Central Nervous System [1]. The study was approved by the Human Research Ethics Committee of Grupo Hospitalar Conceição (4.418.814) and the Federal University of Rio Grande do Sul (3.986.203). Informed consent was obtained for the collection of tissue and blood samples from all patients.

Before surgery, peripheral blood was collected in sodium citrate tubes and tumor tissue samples were divided in two. A piece of the tissue was snap-frozen and stored at  $-80^{\circ}\text{C}$  until RNA extraction. The other part was placed in a sterile conical tube containing DMEM/F-12 (Gibco BRL, USA) with 10% FBS and 0.5 U/mL penicillin/streptomycin (Gibco BRL, USA).

The average time from surgical resection to the beginning of the tissue dissociation protocol was 60 min. Briefly, tumor tissue samples were manually minced into approximately 0.5 to 1 mm diameter pieces using a sterile scalpel followed by enzymatic digestion with collagenase IV (200 U/mL, Sigma-Aldrich, cat: C5138) and DNase I (28 U/mL, cat: AM2224)

in HBSS buffer for 45 min ( $37^{\circ}\text{C}$ , gentle shaking). Dissociation was stopped by adding FBS.

### Establishment and characterization of primary tumor cell cultures

After the dissociation, the isolated cells were resuspended in DMEM/F-12 supplemented with 10% FBS, 0.5 U/mL penicillin/streptomycin, and amphotericin B. Subsequently, cells were seeded in 25  $\text{cm}^2$  culture flasks and maintained at  $37^{\circ}\text{C}$ , minimum relative humidity of 95% and 5%  $\text{CO}_2$  in the air. All cultures were inspected daily using a phase-contrast microscope and the media was changed every two days.

For further characterization and to ascertain whether the primary glioma cell cultures presented similarities to the primary glioma tissue, immunocytochemical staining for GFAP was performed. Briefly,  $10^4$  cells were seeded in 48-well plates. Cells were fixed with 4% paraformaldehyde, permeabilized, and non-specific binding was blocked using a solution containing 10% FBS and 0.1% Triton X100 for 1 h. After, the cells were incubated with the primary antibody anti-GFAP (1:500, Millipore, MAB360) for 1 h (RT), followed by goat anti-mouse Alexa-488 secondary antibody (1:500, Invitrogen, A11001) for 30 min. Nuclei were counterstained with DAPI (300 nM, Sigma-Aldrich, D9542) for 5 min. Images were taken with the EVOS FLoid Imaging System (ThermoFisher, EUA).

### CD39 and CD73 immunocontent

To analyze the CD39 and CD73 protein expression,  $10^6$  cells from primary glioma cell cultures were stained with anti-CD38-FITC (clone: HIT2, cat. 560,982), anti-CD73-PE (clone: AD2, cat. 550,257), and anti-CD39-APC (clone: TU66, cat. 560,239, all from (BD Biosciences, USA) for 30 min on ice and then washed twice. Data was acquired in the BD Accuri™ flow cytometer and analyzed with FlowJo™ Software (BD Biosciences, USA).

### ATP metabolism assay

For ATP hydrolysis assay,  $4 \times 10^4$  cells from primary glioma cell cultures were seeded in 24-well plates until confluence was achieved. After, cells were maintained in a water bath at 37°C and washed with an incubation medium (2 mM  $\text{CaCl}_2$ , 120 mM NaCl, 5 mM KCl, 10 mM glucose, and 20 mM Hepes buffer, pH 7.4). The enzymatic reaction was started by adding 200  $\mu\text{L}$  of incubation medium containing ATP (100  $\mu\text{M}$ ). Cells were incubated for 15, 30, and 60 min and the reaction was stopped on ice. Subsequently, supernatants were centrifuged ( $16,000 \times g$  for 30 min at 4°C) and 20  $\mu\text{L}$  aliquots were applied to a reverse-phase HPLC system (Shimadzu, Japan) using a C18 column (Ultra C18, 25 cm  $\times$  4.6 mm  $\times$  5  $\mu\text{m}$ , Restek, USA). Our protocol was based on a method described previously by Voelter et al. [25] and executed with some adjustments. The elution was performed by applying a gradient from 100% solvent A (60 mM of potassium phosphate monobasic and 5 mM of tetrabutylammonium chloride, pH 6.0) to 100% solvent B (solvent A + 30% of methanol) over 35 min (flow rate: 1.2 mL/min). The amount of each purine was measured by absorbance at 254 nm. Purine standards (50  $\mu\text{M}$ ) were used to evaluate the retention time of each compound separately allowing their identification and quantification. Further, mixes containing the standards were used in different concentrations (1.56–50  $\mu\text{M}$ ) for calibration. The protein concentration was quantified with the Coomassie Blue method, using bovine serum albumin as a control. Purine concentrations were expressed as micromolar ( $\mu\text{M}$ ).

### Isolation of tumor-infiltrated leukocytes and peripheral blood immune cells

After the tumor dissociation, larger cellular aggregates were removed using a cell strainer (40  $\mu\text{m}$ —Falcon®). The strained samples were washed twice with PBS + 2% FBS before flow cytometry analysis. Peripheral blood mononuclear cells (PBMC) were purified with Histo-paque®-1077 (Sigma-Aldrich, USA) density gradient from 10 mL of whole blood collected before the surgery in tubes containing sodium citrate. Plasma was isolated after centrifugation, clarified, and stored at  $-80^\circ\text{C}$ . Erythrocytes from both tumor-infiltrated leukocytes and PBMC were lysed with BD Pharm Lyse buffer (BD Biosciences, USA).

### Flow cytometry of tumor-infiltrated leukocytes and peripheral blood immune cells

After being isolated, tumor-infiltrated leukocytes and PBMC were blocked for non-specific binding using a FACS buffer (Phosphate Buffered Saline + 2% FBS) and stained with the

following panel: CD45-V500 (clone: HI30, cat. 560,777) / CD4-Pacific Blue (clone: RPA-T4, cat. 558,116) / CD39-FITC (clone: TU66, cat. 561,444) / CD73-PE (clone: AD2, cat. 550,257) / CD19-PE-Cy7 (clone: SJ25C1, cat. 557,835) / CD8-APC (clone: RPA-T8, cat. 555,369) / CD38-APCH7 (clone: HB7, cat. 656,646) (BD Biosciences, USA) for 30 min at 4°C. Data was acquired on FACSCanto II (BD Biosciences, USA) flow cytometer and data analysis was performed using FlowJo™ Software (BD Life Sciences, USA). Dead cells were removed from the analysis based on side and forward scatter profiling. The gate was refined on single cells (FSC-A  $\times$  FSC-H).

### Bioinformatics analysis

Determination of gene signatures as well as Kaplan–Meier analyses, considering overall survival as the endpoint, were performed in the Xena platform [26]. The gene signature for B lymphocytes, cytotoxic T lymphocytes, NK cells, and regulatory T lymphocytes was defined based on the median value of gene expression described in the Supplementary Table 2, samples were filtered when presenting higher expression of all genes in the gene set. Furthermore, analyses were performed, after filtering for each gene signature, in relation to the expression of *ENTPDI*, *NT5E*, and *CD38* genes. Furthermore, the expression of these genes was divided into binary categories (high/low), and the Kaplan–Meier analysis was performed as previously determined. The glioblastoma samples used in the analyses were obtained from the TCGA (The Cancer Genome Atlas) from the Glioblastoma (GBM) dataset, while the glioma samples were obtained from the TCGA Lower Grade Glioma (LGG), both through the Xena interface.

### RNA extraction and cDNA synthesis

Total RNA was extracted from  $1 \times 10^6$  cells (primary glioma cell culture) or 50 mg of tumor tissue using TRIzol® reagent according to the manufacturer's instructions (Invitrogen, USA). RNA purity was assessed spectrophotometrically by absorbance at 260/280 nm in a BioPhotometer Plus (Eppendorf, Germany). Complementary DNA (cDNA) was synthesized from 2  $\mu\text{g}$  of total RNA using M-MLV Reverse Transcriptase (Promega Corporation, USA) and stored at  $-20^\circ\text{C}$  until further use.

### Quantitative real-time polymerase chain reaction (qPCR)

All reactions were performed in triplicate using GoTaq® qPCR Master Mix (Promega Corporation, Wisconsin, USA) in a 96-well Real-Time PCR instrument StepOne-Plus™ (Applied Biosystems, USA). The specificity of the

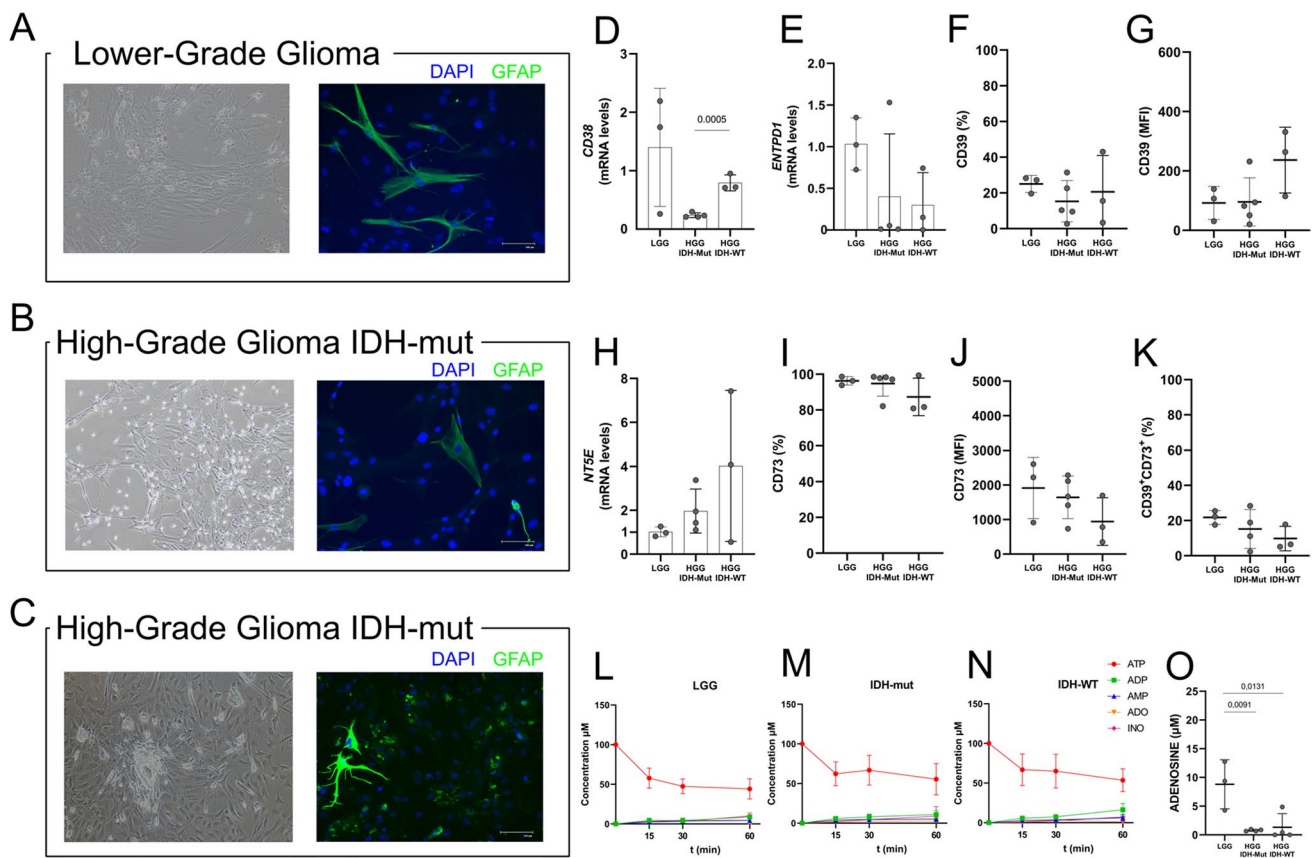


**Fig. 1** Glioma-derived primary cell culture. Representative images of primary cultures derived from different glioma grades. Almost all cells were GFAP positive (some with very low expression, green). DAPI was used to stain the nucleus (blue). Scale bar = 100  $\mu$ m (A–C). No difference between LGG and HGG was observed in primary cell culture regarding CD38, CD39, and CD73 ectoenzymes protein and

mRNA expression (D–K). Cells were incubated with ATP 100  $\mu$ M for 15, 30, and 60 min, and nucleotides and nucleosides metabolism was evaluated by HPLC. LGG cell cultures show a significant increase in ADO production compared to HGG (L–O). The experiment was performed in triplicate using primary cell cultures derived from eleven patients with different glioma grades. Data is shown as the mean  $\pm$  SD

amplified products was confirmed by dissociation curves analyses at the end of each reaction. Gene sequence information was collected ([www.ensembl.org](http://www.ensembl.org) and <https://www.ncbi.nlm.nih.gov/refseq/>) and used to design specific primers for *CD38*, *NT5E*, *ADORA1*, *ADORA2A*, *ADORA2B*, *ADORA3*, *ENTPD1*, *ENTPD3*, *ENPP1*, and *ADA* designed according to Ye et al. [27] and the sequences are provided in Supplementary Table 3. The reactions were performed in triplicate in a final volume of 20  $\mu$ L. We used 2  $\mu$ L of cDNA (50  $\mu$ g) as a template for qPCR reactions and SYBR green as the fluorescent detector. Thermal cycling profile for gene expression consisted of an initial denaturation step at 94  $^{\circ}$ C for 2 min followed by 40 cycles of 15 s at 94  $^{\circ}$ C, 15 s at 60  $^{\circ}$ C and 1 min at 72  $^{\circ}$ C for data acquisition. Sole product amplification and the absence of primer-dimer were confirmed using melting curve analyses at the end of each run. Quantitative data analysis was performed using the  $\Delta\Delta$ Ct method [28]. Values were normalized according to the endogenous control *ACTB* and expressed as relative expression levels.

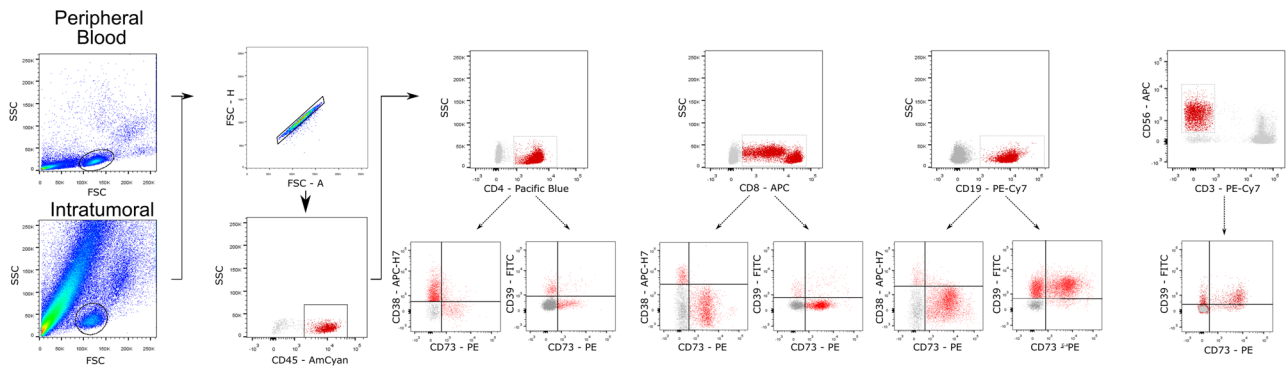
## Plasmatic purine levels

Nucleotides and nucleosides levels in plasma were evaluated by HPLC. Briefly, plasma samples were denatured with 0.6 M perchloric acid. All samples were centrifuged (16,000  $xg$ , 30 min, 4 $^{\circ}$ C) and 4N KOH was used to neutralize the supernatants. A second centrifugation was used to clarify the samples (16,000  $xg$ , 30 min, 4 $^{\circ}$ C). After, purine levels were determined by HPLC as already described in topic 2.3.2. This assay was not performed with recurrent glioma patients' samples.

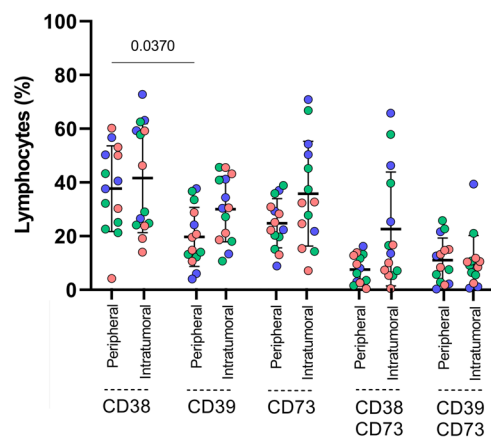
## Statistical analysis

The Shapiro–Wilk test was performed to verify if the analysed data were normally distributed. For data without a normal distribution, a non-parametric test (Kruskal–Wallis), followed by Dunn's post-test, was performed. On the other hand, for data with normal distribution, a parametric test (ANOVA), followed by Tukey post-test was performed.

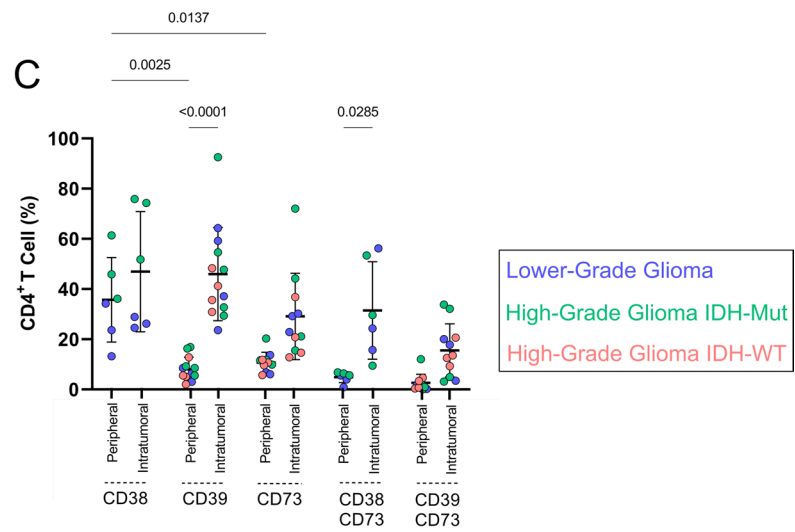
## A Gating Strategy



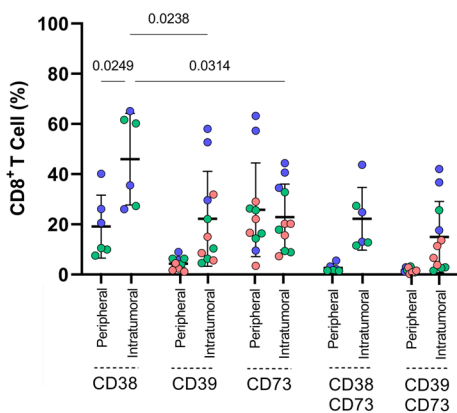
## B



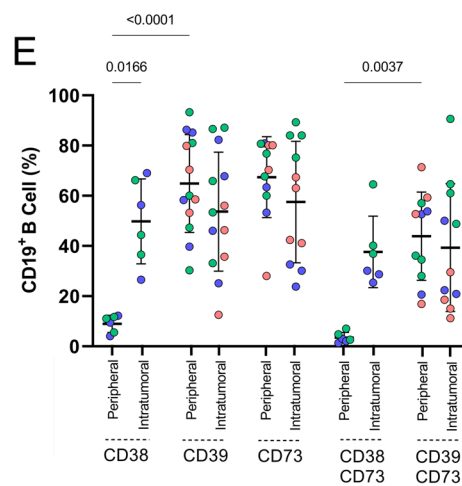
## C



## D



## E



## F

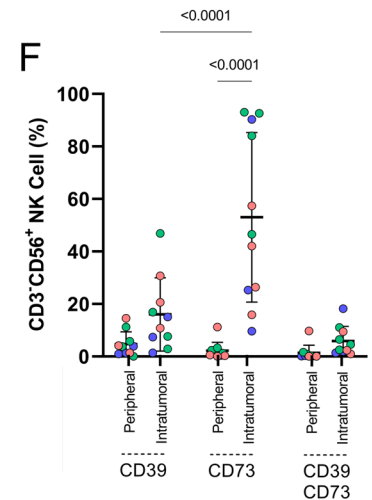


**Fig. 2** Purinergic ectoenzymes are increased in glioma TME regardless of grade. Representative flow cytometry plots detailing the gating strategy to identify purinergic ectoenzymes in NK cells, T and B lymphocytes subsets (A). Tumor-infiltrating immune cells compared with matched patient blood across all tumor grades (II, III, and IV-Mut/

WT) in total lymphocytes (B), CD4+T cells (C), CD8+T cells (D), CD19+B cells (E) and NK cells (F). Data represent a combination of experiments involving individual patients and is displayed as the mean  $\pm$  SD

Analyses were made using GraphPad Prism 9.4.1 software®. Data are expressed as the mean  $\pm$  S.D. Differences were considered significant when  $p < 0.05$ .

## Results

### Characteristics of the analyzed cohort

The study included 28 patients with glioma (Tables 1 and S1), with a mean age of 53.28 years, divided into three grades: five grade II cases (LGG, Diffuse Astrocytoma), two grade III cases (LGG, Anaplastic Astrocytoma) and twenty-one grade IV cases (HGG, GB). Almost half of the patients, 57.14% ( $n=16$ ), had isocitrate dehydrogenase 1 (IDH1) mutation, confirmed by immunohistochemistry. In GB cases, IDH1 mutation was present in 32.14% ( $n=9$ ).

The establishment of primary cell cultures as well as immune analyses using surgical tumor specimens depends on multiple factors, such as the viability of tumor cells (which can be affected by storage, temperature and, previous treatments carried out by patients), and the amount and quality of tumor tissue available. Thus, not all tumors successfully generated a primary cell culture or could be immunologically profiled.

### Glioma-derived primary cell cultures establishment

Cells from 11 glioma cases, comprising three different grades (II, III, and IV) were successfully isolated and cultured (see details in Fig. 1A-C and Table S1). Most of the glioma-derived primary cell culture were morphologically homogeneous, regardless of glioma grade. Furthermore, almost all cells were GFAP positive (some with very low expression), confirming the similarity to the glioma tissue with no fibroblast contamination (Fig. 1A-C).

Despite the markedly low expression, *CD38* mRNA expression is down-regulated in HGG IDH-Mut compared to LGG and HGG IDH-WT (Fig. 1D). All 11 LGG and HGG primary cell cultures were evaluated for CD38, CD39, and CD73 mRNA levels and proteins' surface expression levels. LGG, HGG IDH-Mut, and HGG IDH-WT exhibited very low expression of CD38 (data not shown), and similar expression of *ENTPD1/CD39* (Fig. 1E, F, G) and *NT5E/CD73* (Fig. 1H, I, J), given that CD73 resembles the pattern seen in immortalized GB cell lines [29], with higher expression of this ectoenzyme in comparison to CD39. Although there was no significant difference between the frequency of CD39<sup>+</sup>CD73<sup>+</sup> cells in LGG or HGG cultures (Fig. 1K), we incubated LGG and HGG cells with ATP to evaluate the nucleotides and nucleosides metabolism. As shown in Fig. 1L-N, there was no significant difference in ADP, AMP, and INO production between LGG and HGG primary cell

cultures. Surprisingly, when incubated for 60 min, LGG cells produced more ADO than HGG IDH-Mut and HGG IDH-WT cells (Fig. 1O).

Mutations involving the IDH enzymes are associated with better outcomes in HGG. Hence, we investigated if IDH-Mut or WT HGG-derived cells presented alterations in purinergic ectoenzymes. In line with CD39 and CD73 protein expression (Fig. 1F, G, I, J), both Mut- and WT- HGG cell cultures produced similar concentrations of nucleotides and nucleosides when incubated with ATP (Fig. 1M, N).

### Purinergic ectoenzymes are increased in glioma TME regardless of grade

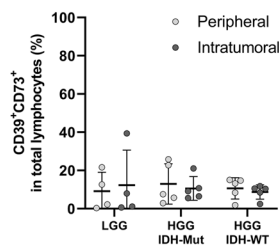
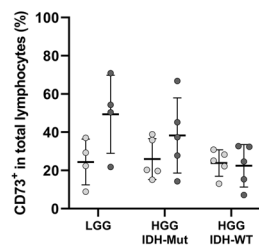
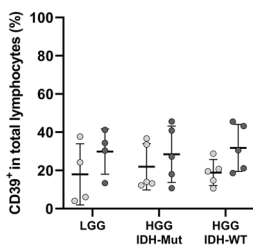
The TME is composed of many cell types, such as cancer cells, endothelial cells, fibroblasts, and immune inflammatory cells. In the tumorigenesis process, tumor-infiltrating immune inflammatory cells play an important role. It has already been well described that CD39 is constitutively expressed in regulatory FoxP3<sup>+</sup> T (Treg) cells [30], while the expression of CD39 in T cytotoxic lymphocytes (CD8<sup>+</sup>) can be related to cell exhaustion [31]. To better understand the purinergic ectoenzymes' roles in glioma-infiltrating lymphocytes, we evaluated the canonical and non-canonical pathways with the expression of CD39 and CD73 in T lymphocytes (CD4<sup>+</sup> and CD8<sup>+</sup>), B lymphocytes (CD19<sup>+</sup>) and NK cells (CD3<sup>-</sup>CD56<sup>+</sup>) in the peripheral blood and infiltrated in the TME of glioma patients. The representative gating strategy is shown in Fig 2A.

First, we evaluated the influence of purinergic ectoenzymes CD38, CD39, and CD73, as well as their coexpression (CD38<sup>+</sup>CD73<sup>+</sup> and CD39<sup>+</sup>CD73<sup>+</sup>), regardless of glioma grade (Fig. 2B-F). Despite not showing differences in total lymphoid cells, T, B, and NK cells, separately, displayed important differences. In the CD4<sup>+</sup> subset, we observed increased CD39<sup>+</sup> and CD38<sup>+</sup>CD73<sup>+</sup> cells intratumorally compared to peripheral blood (Fig. 2C). Interestingly, there was a higher expression of CD38 in CD8<sup>+</sup> and CD19<sup>+</sup> subsets from the tumoral tissue in comparison to peripheral blood (Fig. 2D-E). Also, intratumoral NK cells showed higher CD73 expression (Fig. 2F).

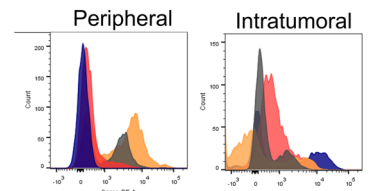
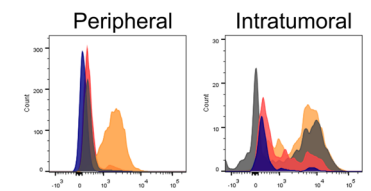
### Influence of CD39-CD73 canonical axis on tumor-infiltrating immune cells from both LGG and HGG

Concerning the total lymphoid population, CD39 and CD73 ectoenzymes expressions are relatively homogeneous when comparing peripheral blood to intratumoral in LGG and HGG (Fig. 3A). However, a deep evaluation of immune cells subpopulations presented important changes in the CD39-CD73 axis in the TME of both LGG and HGG. Regarding T CD4<sup>+</sup> lymphocytes, we observed a significant increase in

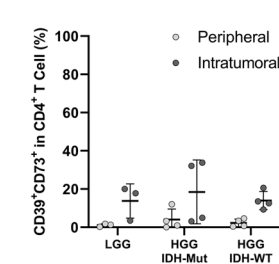
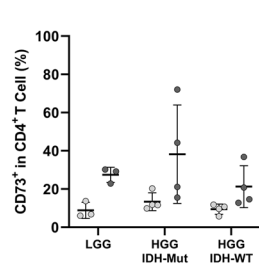
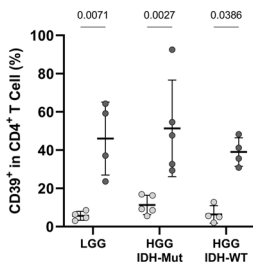
### A Lymphoid Cells



### F Lower-Grade Glioma



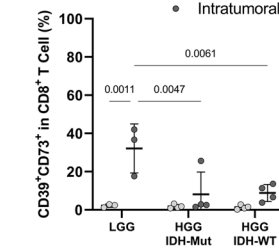
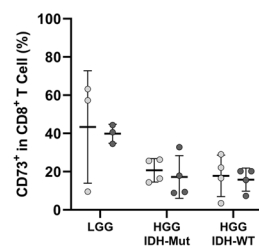
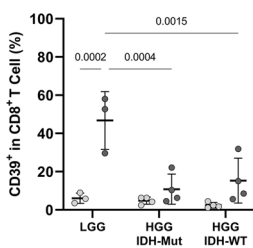
### B CD4+



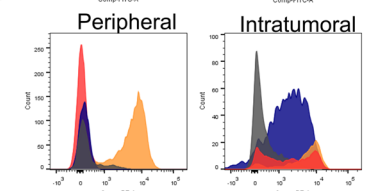
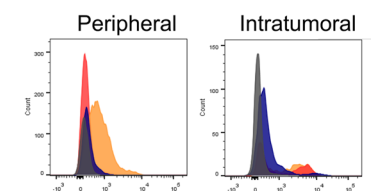
CD39

CD73

### C CD8+



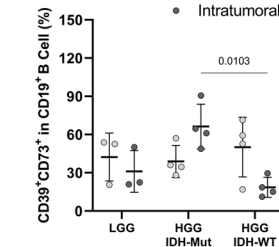
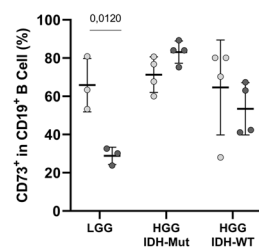
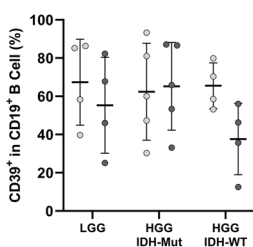
### G High-Grade Glioma IDH-Mut



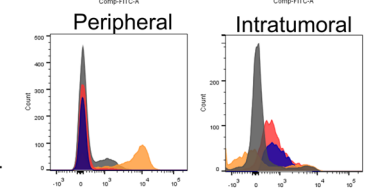
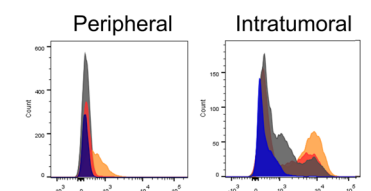
CD39

CD73

### D CD19+



### H High-Grade Glioma IDH-WT



CD39

CD73

### E Natural Killer

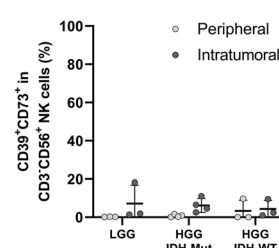
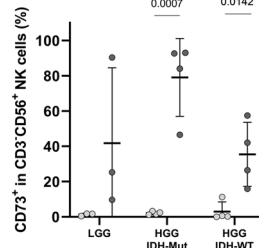
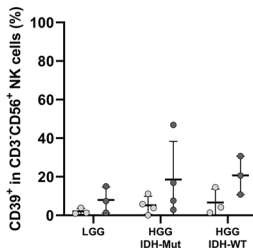




**Fig. 3** CD39-CD73 canonical axis in glioma-infiltrating immune cells compared to matched peripheral blood in LGG, HGG IDH-Mut, and HGG IDH-WT. Percentage of canonical ectoenzymes CD39, CD73, and CD39+CD73+ expression on total lymphocytes (A), CD4+ T cell (B), CD8+ T cell (C), CD19+ B cell (D), and NK (E). Representative histograms highlighting the difference in CD39 and CD73 expression between tumor-infiltrating lymphocytes and peripheral blood in all analyzed groups (F–H). Data represents a combination of experiments involving individual patients and is displayed as the mean  $\pm$  SD

CD39 expression in the intratumoral lymphocytes when compared to the peripheral lymphocytes in both LGG and HGG (Fig. 3B). This increase could be associated with a higher proportion of suppressive CD4<sup>+</sup> cells in the TME. T CD8<sup>+</sup> lymphocytes are, traditionally, associated with cytotoxic activity against tumor cells. Here, we observed significant changes in purinergic ectoenzymes in T CD8<sup>+</sup> cells (Fig. 3C), for example, intratumoral CD39 expression is higher in LGG when compared to HGG (Fig. 3C). CD39 expression in T CD8<sup>+</sup> lymphocytes has already been associated with an exhausted phenotype [31, 32]. CD19<sup>+</sup> B cells expressing CD73 in peripheral blood are similar in both LGG and HGG; however, in LGG we observed a significant reduction in CD73 expression when comparing LGG peripheral blood and HGG intratumoral cells (Fig. 3D). Within the innate and cytotoxic cells, CD73 expression is significantly enriched in NK cells intratumorally in HGG compared to peripheral blood (Fig. 3E). Even though this difference is not present in LGG, we observed a very heterogeneous intratumoral CD73<sup>+</sup> population of NK cells, ranging from 9 – 90% in patients. Some interesting reports relate this CD73 overexpression in infiltrating NK cells to non-cytotoxic regulatory functions [33, 34].

Despite being associated with a better prognosis, IDH-mutant gliomas have been reported to present greater immune evasion and to reduce effector immune cell numbers [35]. Here, we did not observe a significant influence of the IDH mutation in the expression of CD38, CD39, or CD73 in different T cell subsets (Fig. 2B-C). On the other hand, in CD19<sup>+</sup> B cells (Fig. 3D), we observed an important increase in B cells expressing both CD39 and CD73 in HGG-Mut when compared to HGG-WT, which may be associated with higher production of ADO and, consequently, immunosuppression.

Regarding peripheral blood, our results suggest that glioma patients do not show a relevant peripheral immune suppression, with peripheral CD4<sup>+</sup>, CD8<sup>+</sup>, and CD19<sup>+</sup> numbers similar to healthy controls [29]. Also, LGG and HGG patients did not show any difference in the nucleotide and nucleoside concentrations in plasma samples (Fig. S1), although a third part of HGG patients presented high levels of ADO. Representative histograms highlight the robust changes in intratumoral immune cells regarding CD39 and CD73 expression in LGG and HGG (Fig. 3F-H).

## Non-canonical pathway involvement in TME immunosuppression

To determine the expression of CD38, as well as of the CD38-CD73 axis, we evaluated these ectoenzymes expression in both LGG and HGG-Mut patients' peripheral blood and immune TME.

Similarly to CD39-CD73 ectoenzymes, we did not observe any difference in the CD38-CD73 axis between LGG and HGG's peripheral and infiltrating lymphoid cells (Fig. 4A). However, looking at each lymphocyte subpopulation, CD38, as well as CD38-CD73 coexpression, present differential patterns in the TME. In the CD4<sup>+</sup> T-subset, CD38 is overexpressed in HGG intratumorally when compared to LGG (Fig. 4B). Interestingly, intratumoral CD4<sup>+</sup>CD39<sup>+</sup> cells overexpressed CD38 in HGG patients compared to LGG patients. Also, only HGG intratumoral CD4<sup>+</sup>CD39<sup>+</sup> cells overexpressed CD38 compared to peripheral blood, which can enhance ADO production and T cell impairment in HGG patients (Fig. 4B). We observed an important increase in CD38 expression in intratumoral CD8<sup>+</sup> T cells when compared to peripheral blood, in HGG (Fig. 4C). CD38 and CD39 expressions in T CD8<sup>+</sup> lymphocytes have been associated with cellular exhaustion [31, 32], suggesting the presence of dysfunctional T CD8<sup>+</sup> cells. We also noticed a similar immunosuppressor pattern in B lymphocytes (Fig. 4D). CD19<sup>+</sup> B cells expressing CD38, given that this phenotype is attributed to suppressor B cells [19, 36], are significantly increased intratumorally compared to peripheral blood in HGG patients (Fig. 4D). Also, the coexpression of CD38-CD73 in CD8<sup>+</sup> and CD19<sup>+</sup> subsets is increased in both LGG and HGG TMEs. Representative histograms highlight the robust changes in intratumoral immune cells regarding CD38 expression in LGG and HGG (Fig. 4E-F).

Altogether, these results suggest an involvement of lymphocytic purinergic ectoenzymes of both canonical and non-canonical pathways in the immunosuppressive intratumoral microenvironment in LGG and HGG.

## CD38, ENTPD3, A<sub>1</sub>R and A<sub>2A</sub>R genes are upregulated in LGG TME

ADO is an important purine-derived nucleoside produced extracellularly by a complex ectoenzyme network. In the TME, tumor and non-tumor cells communicate dynamically and shape the tumor landscape. The complexity of interactions within the microenvironment cannot be explained solely by tumor cell analysis or immune interactions. It is equally important to evaluate and contemplate all components of this microenvironment. In this sense, multiple TME cells can simultaneously express a variety of related

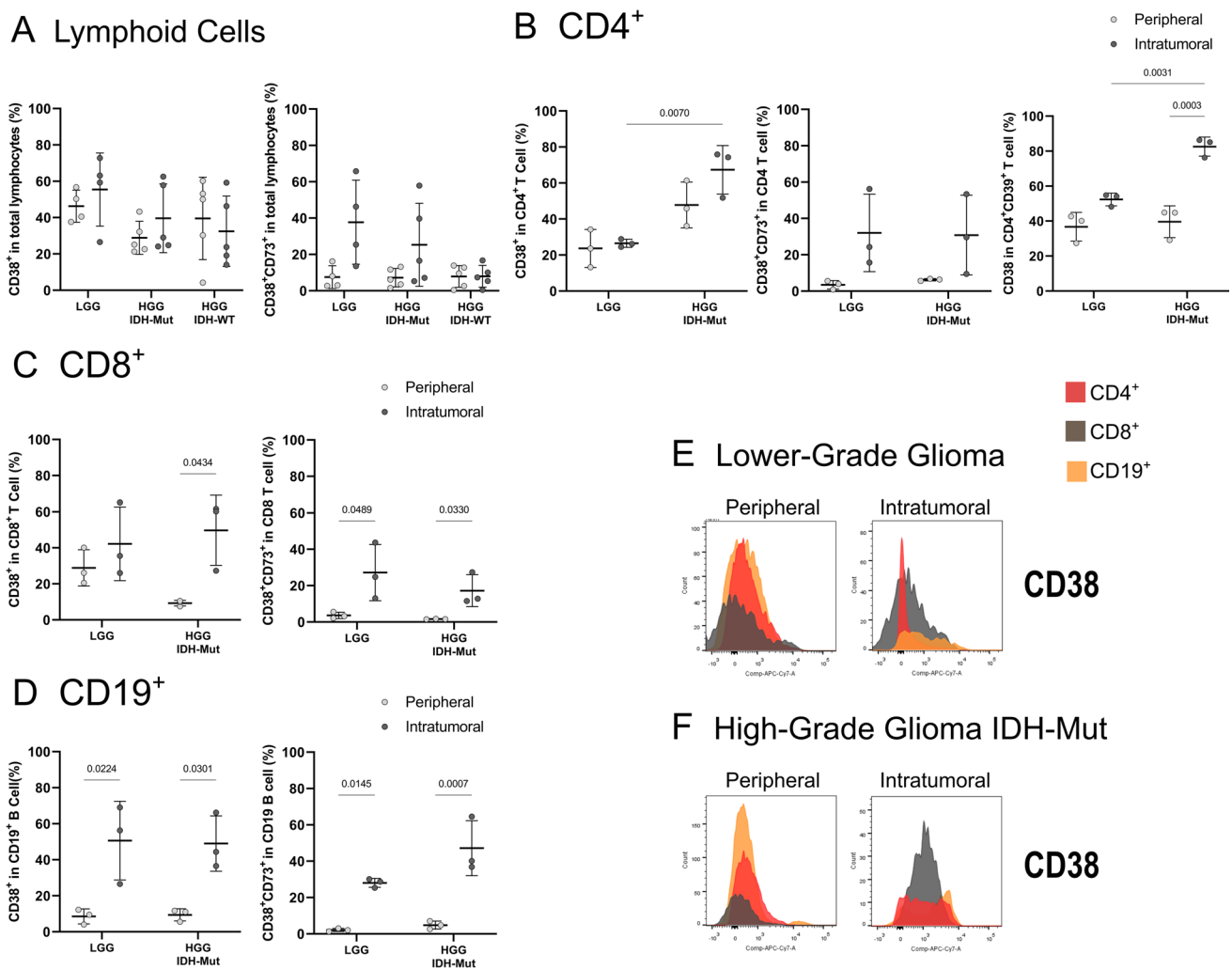


**Fig. 4** CD38-CD73 non-canonical axis in glioma-infiltrating immune cells compared to matched peripheral blood in LGG and HGG IDH-Mut. Percentage of total lymphocytes expressing non-canonical ectoenzyme CD38 and coexpression CD38CD73 (A), CD4<sup>+</sup> T cells (B), CD8<sup>+</sup> T cells (C), and CD19<sup>+</sup> B cells (D). Representative histograms

highlighting the difference in CD38 expression between tumor-infiltrating lymphocytes and peripheral blood in all analyzed groups (E – F). Data represent a combination of experiments involving individual patients and are displayed as the mean  $\pm$  SD

ectoenzymes that can hydrolyze different nucleotides, which in turn can generate multiple different responses. To better characterize the ectoenzymes expressed by tumor samples, we performed qRT-PCR analysis of *ENTPD1* (NTPDase1), *ENTPD3* (NTPDase 3), *NT5E* (CD73), *CD38* (CD38), and *ENPP1* (NPP1) genes. Here, we compared HGG to LGG samples. As illustrated in Fig. 5, qRT-PCR analysis shows that *CD38* and *ENTPD3* are upregulated in LGG when compared to HGG-WT (Fig. 5A, D). Accordingly, both *ENTPD1* and *NT5E* gene expressions are increased in HGG IDH-Mut when compared to IDH-WT (Fig. 5C, E).

Furthermore, we analyzed if mRNA levels from the whole TME are correlated with protein expression from the respective isolated immune infiltrates and found a strong correlation between *CD38* gene and protein expression (Fig. 5K,

$r = 0.6455$ ). This suggests *CD38* gene expression in whole tumor samples is strongly influenced by the immune cell infiltrate, once lymphocytes also presented an increase in CD38 protein expression, as observed in Fig. 2B. In our bioinformatic analyses, LGG patients expressing higher CD38 have better overall survival (OS) rates (Fig. 5Q). Conversely, in LGG patients with high CD8<sup>+</sup> signature, higher CD38 is associated with a better prognosis (Fig. S2J). As observed in our immune TME analysis by flow cytometry, most of the TILs subsets express more purinergic ectoenzymes when compared to peripheral blood, highlighting the importance of TME immune regulation. This regulation may be carried out by many immunoregulatory molecules, such as ADO, through interaction with ADO receptors (AR). To elucidate the expression of ARs in glioma samples, we performed

qRT-PCR of *ADORA<sub>1</sub>*, *ADORA<sub>2A</sub>*, *ADORA<sub>2B</sub>*, and *ADORA<sub>3</sub>* genes. qRT-PCR analyses demonstrated that some of these genes are upregulated in LGG when compared to HGG-WT samples, including *A<sub>1</sub>* and *A<sub>2A</sub>* (Fig. 5F-G). In immune cells, *A<sub>2A</sub>R* portrays an important immunosuppressive role for the TME, inhibiting antitumor response through limiting Teff function and promoting a pro-tumor response by the induction of Treg cells [24, 37, 38].

## Discussion

Intratumor heterogeneity confers an evolutionary advantage and is one of the main causes of treatment failure and tumor relapses [39]. Gliomas are one of the most highly heterogeneous tumors [1]. Therefore, we must comprehend the many ways by which glioma cells interact with the TME, to better understand how these tumors establish and thrive. Currently, several studies have investigated TME components and how they interact with others [14, 16, 40, 41]. The complex cross-talk between cells in the TME strongly relies on the secretion and recognition of several molecules, such as ATP, a powerful damage-associated molecular pattern (DAMP). ATP and ADO are the main agonists of purinergic signaling and support the immunosuppressive glioma milieu [23, 38, 42, 43]. Moreover, the network of ectoenzymes involved in the metabolism of extracellular nucleotides is still highly unexplored in the glioma TME, especially in LGG. Also, differences between IDH-Mut *versus* WT gliomas are still unknown in this context. Recently, Coy and collaborators provide key insights into the significance of immunomodulatory purinergic signaling in HGG patients, focusing on CD39 and CD73. They present interesting results regarding the cell populations interactions within the TME, leading to an increase of ADO levels and poor clinical outcomes [44]. To date, for the first time to our knowledge, this study characterizes glioma TME comparing LGG, HGG IDH-Mut, and HGG IDH-WT patients regarding purinergic canonical and non-canonical pathways, focusing on TILs.

Recent advances in tumor biology oppose the later concept that tumor cells and infiltrating immune cells exert their effects on tumor immunity independently and highlight the complexity of interactions within the microenvironment [45–47]. Our data demonstrate, in coordination with much evidence, that glioma cells, regardless of grade, overexpress CD73 [29, 44, 48], with a low expression of CD39, and a nearly absent expression of CD38, both at protein and mRNA levels. Curiously, LGG-derived primary cell cultures produce more ADO than HGG-derived ones, when incubated with ATP, and this feature must be thoroughly investigated in the future.

In regards to the immune TME profile, we did not observe any differences when assessing the total lymphoid population;

however, we observed an evident increase in all ectoenzymes analyzed in the TME when compared to peripheral blood in each lymphoid subset, pointing out the importance of each cell subtype in the TME. Indeed, the differences in immune TME compared to peripheral blood, in all patients, highlight cells with a potential suppressor phenotype. We believe this favors an immunosuppressive TME due, partially, to extracellular ADO production, regardless of tumor grade. Thus, here we highlight: (1) In healthy brains, the migration of immune cells is tightly regulated. In glioma, the impaired blood–brain barrier allows leukocytes to infiltrate the CNS [49, 50]; (2) correlating the literature, our results suggest that glioma patients do not present a relevant peripheral immune suppression, with peripheral CD4<sup>+</sup>, CD8<sup>+</sup>, and CD19<sup>+</sup> levels similar to healthy controls [29]. Nonetheless, we observed important differences in the intratumoral immune compartment. For example, the CD4<sup>+</sup> T cell subset, in which glioma patients overexpress CD39. It has been described that CD39 supports the suppressive function of Tregs [30, 48, 51, 52] and it is commonly increased in many tumors, promoting pro-tumoral immune response, ADO production, and IL-10 release, hence immunosuppressing the TME. Some studies correlate the increase of intratumoral Tregs and higher glioma grades [53, 54]. In contrast, we did not observe any differences regarding CD4<sup>+</sup>CD39<sup>+</sup> cells between grades, suggesting similar immunosuppression levels related to the CD4<sup>+</sup>CD39<sup>+</sup> phenotype. On the other hand, a recently discovered NK population that overexpresses CD73 and presents a suppressor phenotype, with increased production of ADO and IL-10, is significantly increased only in HGG immune TME comparing to LGG [33, 55]. These dysfunctional NK cells possibly support a stronger TME immunosuppression in HGG patients.

Interestingly, in the canonical pathway, more differences between LGG and HGG TME emerge, mainly in CD8<sup>+</sup> T cells and CD19<sup>+</sup> B cells. Moreover, LGG presented higher CD39 expression in intratumoral CD8<sup>+</sup> T cells compared to HGG, independently of IDH status. Some studies have shown that CD39 is a marker of tumor-specific T cells [56]. Indeed, convergent evidence indicates CD39 expression as a marker of T cell exhaustion in melanoma, carcinoma, colorectal, lung, and breast cancer [31, 57, 58]. Canale et al. [31] showed this cellular phenotype produces decreased amounts of TNF- $\alpha$  and IL-2, besides expressing coinhibitory receptors and inhibiting CTLs IFN- $\gamma$  secretion. Also, Simoni et al. [58] found that CD39<sup>+</sup>CD8<sup>+</sup> TILs present enriched gene expression related to cell proliferation and exhaustion, characteristics of chronically stimulated T cells, [59, 60]. We hypothesize that, in LGG, which comprises mainly younger patients with better prognosis, CTLs become activated to kill tumor cells and, due to tumor immune evasion mechanisms, might become exhausted later on. This, associated with an increase in T CD8<sup>+</sup> cells coexpressing CD39-CD73 in LGG intratumorally, might

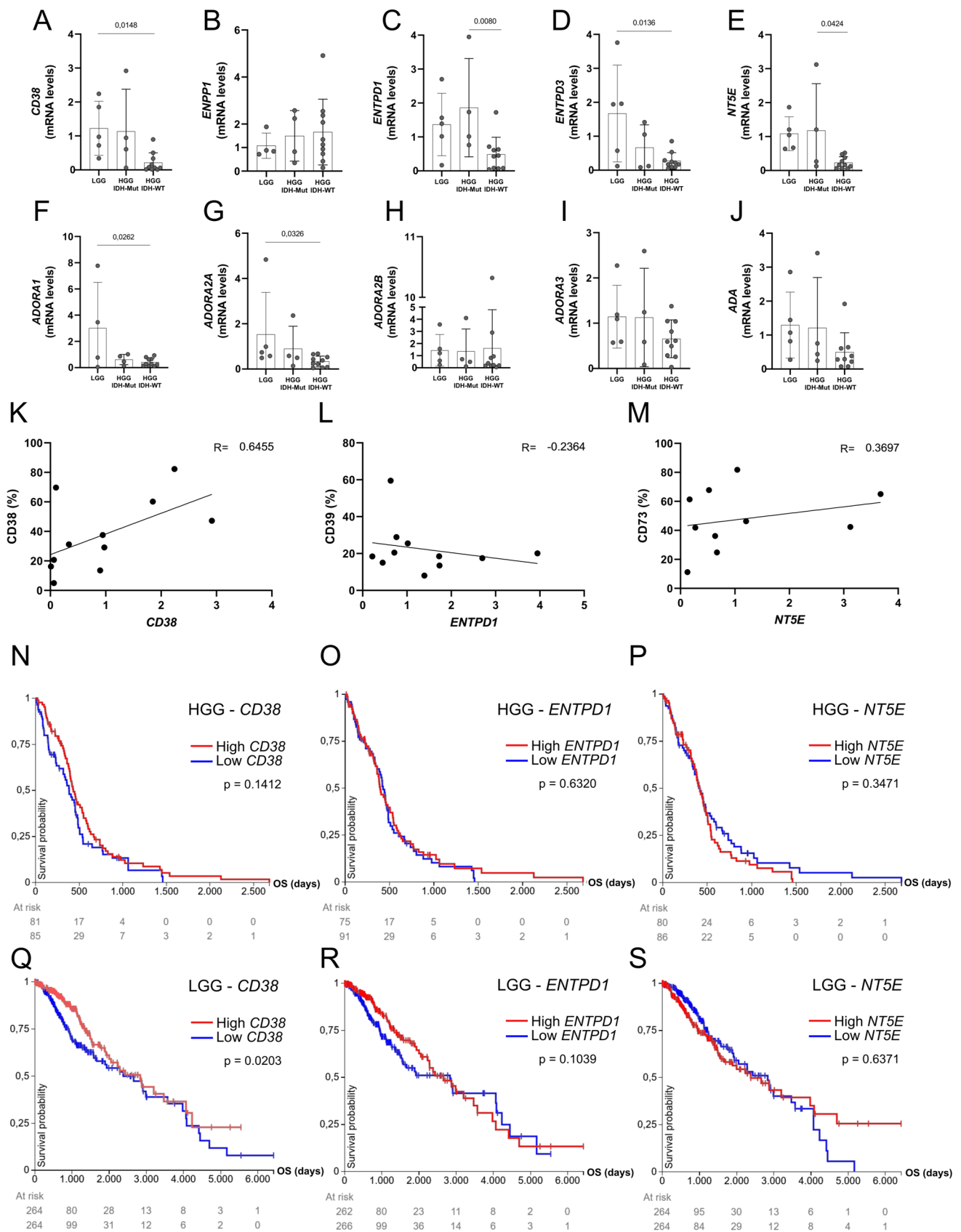


**Fig. 5** Purinergic ectoenzymes (A – E; J) and adenosinergic receptors (F – I) gene expression were evaluated by qRT-PCR and HGG tumor samples were compared to LGG. Graphs show the correlation between the percentage of CD38<sup>+</sup> tumor-infiltrating lymphocytes and CD38 mRNA expression from tumor sample (K), the percentage of CD39<sup>+</sup> tumor-infiltrating lymphocytes and *ENTPD1* mRNA expression from tumor sample (L), and the percentage of CD73 tumor-infiltrating lymphocytes and *NT5E* mRNA expression from tumor sample (M), regardless the tumor grade. Kaplan–Meier analysis showing the influence of *CD38*, *ENTPD1*, and *NT5E* genes expressions on HGG and LGG OS (N – S). Data represent a combination of experiments involving individual patients and are displayed as a single value by the Spearman test

produce important immunosuppression in the TME, with impaired production of proinflammatory cytokines, such as IFN- $\gamma$ , TNF- $\alpha$ , IL-2, and high production of ADO, IL-10, and TGF- $\beta$ . In contrast, some studies attribute CD39<sup>+</sup>CD8<sup>+</sup> TILs, mostly presenting CD103 co-expression, to an effector phenotype and better prognosis [61–63]. Furthermore, LGG intratumoral CD19<sup>+</sup> B cells present a lower CD73 expression compared to peripheral blood and HGG-Mut intratumoral cells. B-cells have been overlooked in the oncoimmunology field. Evidence suggests that there are different functional subsets of B cells, acting both suppressing or enhancing T-cell responses [19, 64, 65]. Also, a few studies observed CD73 expression in human B cells [19, 66]. Saze et al. [66] has shown that activated B cells present lower CD73 expression when compared to naïve B cells, producing more AMP than ADO. In this context, we believe that intratumoral LGG B cells might produce less ADO than HGG ones, turning to be highly immunosuppressive later on when comparing to LGG.

As a surface receptor, CD38 is necessary for immune cell activation and proliferation and is highly expressed on activated T, B, NK, and myeloid-derived suppressor cells [67], showing a strong immunosuppressive role in many types of cancer [32, 68]. In our cohort, we observed a strong correlation between CD38 protein expression in TILs and whole TME mRNA levels. Our results demonstrate an important intratumoral upregulation of CD38, and CD38<sup>+</sup>CD73<sup>+</sup> co-expressing cells, in both T CD8<sup>+</sup> and B cells. Generally, CD38 expression is related to impaired and suppressor responses via ADO in many cancers [32, 69, 70]. Chen et al. [71], showed a small subset of CD8<sup>+</sup> cells, expressing CD38 and HLA-DR, being upregulated in HGG and presenting an effector function due to strong IFN- $\gamma$  and IL-2 secretion. Curiously, this subset also presented an increase in PD-1 expression, which is a known promoter of cellular exhaustion [71]. However, Zhang et al. [32] showed an increase of those CD38<sup>+</sup>CD8<sup>+</sup> T cells in metastatic pleural effusions compared to matched PBMCs. This CD8<sup>+</sup> subset can present an impaired IFN- $\gamma$  and TNF- $\alpha$  production capacity and PD-1 upregulation, contributing to an exhausted phenotype [32]. Indeed,

CD38 has been associated with regulatory functions. It has been observed in many cancer types that CD38<sup>high</sup> Breg cells produce IL-10, and inhibit T effector cells while supporting Treg proliferation [36, 72, 73]. Here we showed that CD38, as well as CD38-CD73, are overexpressed in intratumoral CD19<sup>+</sup> B cells when compared to peripheral blood, suggesting an immunosuppressive role for B cells in the TME of both LGG and HGG. Furthermore, CD38 expression on CD4<sup>+</sup> Tregs has been associated with higher suppressive activity, and the capacity to upregulate CD73 [74, 75]. Indeed, in our study, intratumoral CD4<sup>+</sup>CD39<sup>+</sup> cells overexpressed CD38 in HGG patients compared to LGG patients. Also, only HGG intratumoral CD4<sup>+</sup>CD39<sup>+</sup> cells overexpressed CD38 compared to peripheral blood, which can enhance ADO production and T cell impairment in HGG patients. Altogether, the emerging evidence related to CD38, found by us and others [69, 72, 75], indicates a multi-faceted immunosuppressive role for this ectoenzyme in regulating the TME.

One of the most important markers that distinguish LGG from HGG is the IDH mutational status. Most LGG patients harbor IDH mutations compared to few HGG [1]. In this study, all LGG samples were IDH-Mut, whereas 32% of HGG were IDH-Mut. Indeed, in our study, the main differences observed were between LGG patients, which are all IDH-Mut, and HGG IDH-WT, bringing forth the relevance of this mutation for glioma progression. Furthermore, *CD38*, *NTPDase3*, *AIR*, and *A2AR* gene expressions were upregulated in LGG tumor samples when compared to HGG IDH-WT. In the literature, most of the data are related to CD38 protein expression in the immune TME. Our findings show upregulation of *CD38* in LGG samples of a Brazilian cohort, which is corroborated by LGG *versus* GBM results from TCGA [76], Perenkov et al. [77], Chmielewski et al. [78], and Zhu et al. [79] where high expression of *CD38* correlates with early disease stage in LGG [76], colorectal [77], prostate [78], and ovarian cancer [79], respectively. This upregulation in lower-grade tumors is associated with a better prognosis in some studies [79], [80] as well as in our bioinformatic analyses, in which better overall survival is seen in LGG patients expressing higher CD38. Additionally, the upregulation of *ENTPD3* in lower grades was also observed in bladder cancer [81, 82]. The difference between LGG and HGG IDH-WT in *CD38* and *ENTPD3* expression could be related to the loss of expression of both genes (probably in non-immune cells) throughout tumor progression and staging increase [77, 80]. Interestingly, we found some contrasting results regarding A<sub>1</sub>R and A<sub>2A</sub>R. Although literature still lacks information regarding ADO receptors expression and activity in LGG, Huang et al. [82] showed that both *AIR* and *A2AR* were expressed at low levels in glioma grades I and II and in high levels in glioma grades III and IV, especially in grade III astrocytoma [82].

Considering that our LGG cohort comprises both grades II and III, the upregulation observed in both receptors, compared to HGG IDH-WT, could have been influenced equally by both groups and the overexpression of these ADO receptors might induce immune responses for tumor evasion [83]. Grades II and III are often collectively grouped as LGG, notwithstanding there is meaningful heterogeneity among these grades regarding pathological features and clinical outcomes. Regarding GB patients, the most important difference between IDH status was related to *CD73/NT5E* and *CD39/NTPD1*. The higher expression of both genes in HGG IDH-Mut patients is curious, once it has been well-defined that their overexpression is related to poor prognosis [29, 84]. Indeed, *CD73* overexpression correlates with chemoresistance via  $A_2BR$  [85–87], even though IDH-Mut tumors usually have a better response to chemotherapy [12]. Ott et al. [88] also observed an increase in *CD73* expression in IDH-Mut tumors and, mechanistically, showed this upregulation is induced by the oncometabolite 2-hydroxyglutarate [88]. This oncometabolite is also related to the impairment of T cell response in GBM [89, 90].

We highlight that sample size was the most important limitation of this study. A larger and more diverse sample, mainly in the LGG group, could have enhanced power to detect more differences between the groups. Also, the difficulty to obtain comparative normal brain tissue samples should be considered and our findings should be interpreted with this limitation in mind. We also highlight that this is, mainly, research focused on the characterization of the main purinergic ectoenzymes of canonical and non-canonical pathways in lymphoid cells. However, we consider the absence of deep functional and phenotypical analysis as a limitation of the work.

Altogether, our immune TME results highlight differences between LGG and HGG patients regarding the expression of *CD38*, *CD39*, and *CD73* ectoenzymes, suggesting an increase in immunosuppressive-related markers in the intratumoral compartment, mainly in HGG patients. This could be a contributor to the worse prognosis often seen in HGG patients. However, it is important to highlight these changes may not be enough to switch the immune system towards immunosuppression. Finally, a complex cascade of interactions between all TME cells working synergistically is necessary to promote immunosuppression. Indeed, Takenaka et al., demonstrated that *CD39* expression in TAMs increases ADO production in the TME, leading to T cell dysfunction [84]. This highlights that purinergic signaling is a relevant contributor to tumor immune suppression, which in turn contributes to worse prognosis, treatment response, and patient outcome. Therefore, purinergic ectoenzymes should be perceived as interesting targets in the TME for future glioma and glioblastoma research.

**Supplementary Information** The online version contains supplementary material available at <https://doi.org/10.1007/s11302-023-09931-4>.

**Acknowledgements** The authors would like to thank all the patients who have agreed to participate in this study and their families. We also thank all from Departamento de Neurocirurgia team (Hospital Cristo Redentor) for their work and collaboration, and all our collaborators for the technical support provided. Finally, we thank the funding agencies Coordenação de Aperfeiçoamento de Pessoal de Nível Superior (CAPES), Conselho Nacional de Desenvolvimento Científico e Tecnológico (CNPq), Fundação de Amparo à Pesquisa do Estado do Rio Grande do Sul (FAPERGS) and Instituto Nacional de Ciência e Tecnologia (INCT).

**Author contributions** **Conceptualization:** Juliete Nathali Scholl, Fabrício Figueiró; **Methodology:** Juliete Nathali Scholl, Augusto Ferreira Weber, Camila Kehl Dias, Vinícius Pierdoná Lima, Lucas Kich Grun, Diego Zambonin, Eduardo Anzolin, Wanderson Willian Dos Santos Dias, Willian Pegoraro Kus; **Validation:** Juliete Nathali Scholl, Augusto Ferreira Weber, Camila Kehl Dias, Vinícius Pierdoná Lima; **Formal analysis and Investigation:** Juliete Nathali Scholl, Augusto Ferreira Weber, Camila Kehl Dias, Vinícius Pierdoná Lima; **Writing—original draft:** Juliete Nathali Scholl; **Writing—review & editing:** Juliete Nathali Scholl, Augusto Ferreira Weber, Camila Kehl Dias, Vinícius Pierdoná Lima, Lucas Kich Grun, Diego Zambonin, Eduardo Anzolin, Wanderson Willian Dos Santos Dias, Willian Pegoraro Kus, Florencia Barbé-Tuana, Ana Maria Oliveira Battastini, Paulo Valdeci Worm, Fabrício Figueiró; **Visualization:** Juliete Nathali Scholl; **Supervision:** Fabrício Figueiró; **Project administration:** Juliete Nathali Scholl, Fabrício Figueiró; **Funding acquisition:** Juliete Nathali Scholl, Fabrício Figueiró.

**Funding** This study was supported by Conselho Nacional de Desenvolvimento Científico e Tecnológico (CNPq; n° 406035/2021–0 and PQ n° 311580/2021–1, Figueiró F), Fundação de Amparo à Pesquisa do Estado do Rio Grande do Sul (FAPERGS/PQG grant no. 21/2551–0001972-7) and Instituto Nacional de Ciência e Tecnologia—INCT/CNPq/CAPES/FAPERGS grant no. 465671/2014–4). This study was financed in part by the Conselho Nacional de Desenvolvimento Científico e Tecnológico (CNPq; 140977/2019–8).

**Data availability** All data generated or analysed during this study are included in this published article [and its supplementary information files].

## Declarations

**Competing interests** The authors have no relevant financial or non-financial interests to disclose.

**Conflicts of interest** Juliete Nathali Scholl declares that she has no conflict of interest.

Augusto Ferreira Weber declares that he has no conflict of interest.

Camila Kehl Dias declares that she has no conflict of interest.

Vinícius Pierdoná Lima declares that he has no conflict of interest.

Lucas Kich Grun declares that he has no conflict of interest.

Diego Zambonin declares that he has no conflict of interest.

Eduardo Anzolin declares that he has no conflict of interest.

Wanderson Willian Dos Santos Dias declares that he has no conflict of interest.

Willian Pegoraro Kus declares that he has no conflict of interest.

Florencia Barbé-Tuana declares that she has no conflict of interest.

Ana Maria Oliveira Battastini declares that she has no conflict of interest.

Paulo Valdeci Worm declares that he has no conflict of interest.

Fabrício Figueiró declares that he has no conflict of interest.

**Ethics approval** The study was conducted in accordance with the 1964 Helsinki Declaration, and the protocol was approved by the Ethics Committee of the Grupo Hospitalar Conceição and the Universidade Federal do Rio Grande do Sul (Project n°: 4.343.931, CAAE n°: 24997119.8.3002.5530; and Project number: 3.986.203, CAAE number: 24997119.8.0000.5347).

**Consent to participate** Informed consent was obtained from all individual participants included in the study.

## References

- Louis DN, Perry A, Wesseling P, Brat DJ, Cree IA, Figarella-Branger D, Hawkins C, Ng HK, Pfister SM, Reifenberger G, Soffietti R, Deimling A, Ellison DW (2021) The 2021 WHO Classification of Tumors of the Central Nervous System: a summary. *Neuro Oncol* 23:1231–1251. <https://doi.org/10.1093/neuonc/noab106>
- Furnari FB, Fenton T, Bachoo RM, Mukasa A, Stommel JM, Stegh A, Hahn WC, Ligon KL, Louis DN, Brennan C, Chin L, DePinho RA, Cavenee WK (2007) Malignant astrocytic glioma: Genetics, biology, and paths to treatment. *Genes Dev*. <https://doi.org/10.1101/gad.1596707>
- Zou P, Xu H, Chen P, Yan Q, Zhao L, Zhao P, Gu A (2013) IDH1/IDH2 mutations define the prognosis and molecular profiles of patients with gliomas: a meta-analysis. *PLoS One* 8(7):e68782. <https://doi.org/10.1371/journal.pone.0068782>
- Kang MR, Kim MS, Oh JE, Kim YR, Song SY, Seo SI, Lee JY, Yoo NJ, Lee SH (2009) Mutational analysis of IDH1 codon 132 in glioblastomas and other common cancers. *Int J Cancer* 125(2):353–355. <https://doi.org/10.1002/ijc.24379>
- Montalban-Bravo G, DiNardo CD (2018) The role of IDH mutations in acute myeloid leukemia. *Future Oncol* 14(10):979–993. <https://doi.org/10.2217/fon-2017-0523>
- Wood LD et al (2007) The genomic landscapes of human breast and colorectal cancers. *Science* 318(5853):1108–1113. <https://doi.org/10.1126/science.1145720>
- Vuong HG, Ngo TNM, Dunn IF (2021) Prognostic importance of IDH mutations in chondrosarcoma: An individual patient data meta-analysis. *Cancer Med* 10(13):4415–4423. <https://doi.org/10.1002/cam4.4019>
- Ghiam AF, Cairns RA, Thoms J, Dal Pra A, Ahmed O, Meng A, Mak TW (2012) Bristow RG (2012) IDH mutation status in prostate cancer. *Oncogene* 31(33):3826. <https://doi.org/10.1038/onc.2011.546>
- Shibata T, Kokubu A, Miyamoto M, Sasajima Y, Yamazaki N (2011) Mutant IDH1 confers an in vivo growth in a melanoma cell line with BRAF mutation. *Am J Pathol* 178(3):1395–1402. <https://doi.org/10.1016/j.ajpath.2010.12.011>
- Dang L, White DW, Gross S, Bennett BD, Bittinger MA, Driggers EM, Fantin VR, Jang HG, Jin S, Keenan MC, Marks KM, Prins RM, Ward PS, Yen KE, Liao LM, Rabinowitz JD, Cantley LC, Thompson CB, Heiden MG, Su SM (2009) Cancer-associated IDH1 mutations produce 2-hydroxyglutarate. *Nature* 462(7274):739–744. <https://doi.org/10.1038/nature08617>
- Carbonneau M et al (2016) The oncometabolite 2-hydroxyglutarate activates the mTOR signalling pathway. *Nat Commun* 7:12700. <https://doi.org/10.1038/ncomms12700>
- Houillier C, Wang X, Mokhtari K, Guillemin R, Laffaire J, Paris S, Boisselier B, Idbaih A, Laigle-Donadey F, Hoang-Xuan K, Sanson M, Delattre JY (2010) IDH1 or IDH2 mutations predict longer survival and response to temozolomide in low-grade gliomas. *Neurology* 75(17):1560–1566. <https://doi.org/10.1212/WNL.0b013e3181f96282>
- Richardson LG, Choi BD, Curry WT (2019) (R)-2-hydroxyglutarate drives immune quiescence in the tumor microenvironment of IDH-mutant gliomas. *Transl Cancer Res* 8(2):S167–S170. <https://doi.org/10.21037/tcr.2019.01.08>
- Schiffer D, Annovazzi L, Casalone C, Corona C, Mellai M (2019) Glioblastoma: Microenvironment and niche concept. *Cancers*. <https://doi.org/10.3390/cancers11010005>
- Gargini R, Segura-Collar B, Sánchez-Gómez P (2020) Cellular Plasticity and Tumor Microenvironment in Gliomas: The Struggle to Hit a Moving Target. *Cancers (Basel)* 12(6). <https://doi.org/10.3390/cancers12061622>
- De Vleeschouwer S, Bergers G (2017) Glioblastoma: to target the tumor cell or the microenvironment? Ed., Codon Publications, Chapter 16. Brisbane, Australia. <https://doi.org/10.15586/codon.glioblastoma.2017.ch16>
- Knocke S, Fleischmann-Mundt B, Saborowski M, Manns MP, Kuhnel F, Wirth TC, Woller N (2016) Tailored Tumor Immunogenicity Reveals Regulation of CD4 and CD8 T Cell Responses against Cancer. *Cell Rep* 17(9):2234–2246. <https://doi.org/10.1016/j.celrep.2016.10.086>
- Gieryng A, Psczolkowska D, Walentyłowicz KA, Rajan WD, Kaminska B (2017) Immune microenvironment of gliomas. *Lab Invest* 97(5):498–518. <https://doi.org/10.1038/labinvest.2017.19>
- Figueiró F, Muller L, Funk S, Jackson EK, Battastini AMO, Whiteside TL (2016) Phenotypic and functional characteristics of CD39high human regulatory B cells (Breg). *Oncoimmunology* 5 <https://doi.org/10.1080/2162402X.2015.1082703>
- Schuler PJ, Saze Z, Hong CS, Muller L, Gillespie DG, Cheng D, Harasymczuk MM, Lang S, Jackson EK, Whiteside TL (2014) Human CD4<sup>+</sup> CD39<sup>+</sup> regulatory T cells produce adenosine upon co-expression of surface CD73 or contact with CD73<sup>+</sup> exosomes or CD73<sup>+</sup> cells. *Clin Exp Immunol* 177(2):531–543. <https://doi.org/10.1111/cei.12354>
- Bavaresco L, Bernardi A, Braganhol E, Cappellari AR, Rockenbach L, Farias PF, Wink MR, Delgado-Canedo A, Battastini AMO (2008) The role of ecto-5′nucleotidase/CD73 in glioma cell line proliferation. *Mol Cell Biochem* 319(1):61–68. <https://doi.org/10.1007/s11010-008-9877-3>
- Horenstein AL, Chillemi A, Zaccarello G, Bruzzone S, Quarona V, Zito A, Serra S, Malavasi F (2013) A CD38/CD203A/CD73 ectoenzymatic pathway independent of CD39 drives a novel adenosinergic loop in human T lymphocytes. *Oncoimmunology* 2(9):1–14. <https://doi.org/10.4161/onci.26246>
- Di Virgilio F, Adinolfi E (2017) Extracellular purines, purinergic receptors and tumor growth. *Oncogene* 36(3):293–303. <https://doi.org/10.1038/onc.2016.206>
- Ohta A, Ohta A, Madasu M, Kini R, Subramanian M, Goel N, Sitkovsky M (2009) A2A adenosine receptor may allow expansion of T cells lacking effector functions in extracellular adenosine-rich microenvironments. *J Immunol* 183(9):5487–5493. <https://doi.org/10.4049/jimmunol.0901247>
- Voelter W, Zech K, Arnold P, Ludwig G (1980) Determination of selected pyrimidines, purines and their metabolites in serum and urine by reversed-phase ion-pair chromatography. *J Chromatogr* 199:345–354. [https://doi.org/10.1016/s0021-9673\(01\)91386-x](https://doi.org/10.1016/s0021-9673(01)91386-x)
- Goldman MJ, Craft B, Hastie M, Repecka K, McDade F, Kamath A, Banerjee A, Luo Y, Rogers D, Brooks AN, Zhu J, Haussler D (2020) Visualizing and interpreting cancer genomics data via the Xena platform. *Nat Biotechnol* 38(6):675–678. <https://doi.org/10.1038/s41587-020-0546-8>
- Ye J, Coulouris G, Zaretskaya I, Cutcutache I, Rozen S, Madden TL (2012) Primer-BLAST: a tool to design target-specific primers for polymerase chain reaction. *BMC Bioinformatics* 13:134. <https://doi.org/10.1186/1471-2105-13-134>

28. Schmittgen TD, Livak KJ (2008) Analyzing real-time PCR data by the comparative C(T) method. *Nat Protoc* 3(6):1101–1108. <https://doi.org/10.1038/nprot.2008.73>
29. Xu S, Shao QQ, Sun JT, Yang N, Xie Q, Wang DH, Huang QB, Huang B, Wang XY, Li XG, Qu X (2013) Synergy between the ectoenzymes CD39 and CD73 contributes to adenosinergic immunosuppression in human malignant gliomas. *Neuro Oncol* 15(9):1160–1172. <https://doi.org/10.1093/neuonc/not067>
30. Borsellino G, Kleinewietfeld M, Mitri DD, Sternjak A, Diamantini A, Giometto R, Hopner S, Centonze D, Bernardi G, Dell'Acqua ML, Rossini PM, Battistini L, Rotzschke O, Falk K (2007) Expression of ectonucleotidase CD39 by Foxp3 Treg cells: hydrolysis of extracellular ATP and immune suppression. *Blood* 110(4):1225–1233. <https://doi.org/10.1182/blood-2006-12-064527>
31. Canale FP, Ramello MC, Nuñez N, Furlan CLA, Bossio SN, Serran MG, Boari JT, Castillo AD, Ledesma M, Sedlik C, Piaggio E, Gruppi A, Rodriguez EAA, Montes CL (2018) CD39 Expression Defines Cell Exhaustion in Tumor-Infiltrating CD8(+) T Cells. *Cancer Res* 78(1):115–128. <https://doi.org/10.1158/0008-5472.CAN-16-2684>
32. Zhang Y, Li W, Ma K, Zhai J, Jin Y, Zhang L, Chen C (2022) Elevated CD38 expression characterizes impaired CD8+ T cell immune response in metastatic pleural effusions. *Immunol Lett* 245:61–68. <https://doi.org/10.1016/j.imlet.2022.04.003>
33. Neo SY et al (2020) CD73 immune checkpoint defines regulatory NK cells within the tumor microenvironment. *J Clin Invest* 130(3):1185–1198. <https://doi.org/10.1172/JCI128895>
34. Close HJ, Stead LF, Nsengimana J, Reilly KA, Droop A, Wurdak H, Mathew RK, Corns R, Newton-Bishop J, Melcher AA, Short SC, Cook GP, Wilson EB (2020) Expression profiling of single cells and patient cohorts identifies multiple immunosuppressive pathways and an altered NK cell phenotype in glioblastoma. *Clin Exp Immunol* 200(1):33–44. <https://doi.org/10.1111/cei.13403>
35. Yan Y, Li W, Liu Q, Yang K (2022) Advances in Immune Microenvironment and Immunotherapy of Isocitrate Dehydrogenase Mutated Glioma. *Front Immunol* 13. <https://doi.org/10.3389/fimmu.2022.914618>
36. Domínguez-Pantoja M, Lopez-Herrera G, Romero-Ramirez H, Santos-Argumedo L, Chavez-Rueda AK, Hernandez-Cueto A, Flores-Munoz M, Rodriguez-Alba JC (2018) CD38 protein deficiency induces autoimmune characteristics and its activation enhances IL-10 production by regulatory B cells. *Scand J Immunol* 87(6):e12664. <https://doi.org/10.1111/sji.12664>
37. Gessi S, Merighi S, Sacchetto V, Simioni C (1808) Borea PA (2011) Adenosine receptors and cancer. *Biochim Biophys Acta - Biomembr* 5:1400–1412. <https://doi.org/10.1016/j.bbmem.2010.09.020>
38. Ohta A, Gorelik E, Prasad SJ, Ronchese F, Lukashev D, Wong MKK, Huang X, Caldwell S, Liu K, Smith P, Chen JF, Jackson EK, Apasov S, Abrams S, Sitkovsky M (2006) A2A adenosine receptor protects tumors from antitumor T cells. *Proc Natl Acad Sci U S A* 103(35):13132–13137. <https://doi.org/10.1073/pnas.0605251103>
39. Inda MDM, Bonavia R, Seoane J (2014) Glioblastoma multiforme: a look inside its heterogeneous nature. *Cancers (Basel)* 6(1):226–239. <https://doi.org/10.3390/cancers6010226>
40. Liu Z, Meng Q, Bartek J, Poirot T, Persson O, Rane L, Rangelova E, Illies C, Peredo IH, Luo X, Rao MV, Robertson RA, Dodoo E, Maeurer M (2017) Tumor-infiltrating lymphocytes (TILs) from patients with glioma. *Oncimmunology* 6(2). <https://doi.org/10.1080/2162402X.2016.1252894>
41. DeCordova S, Shastri A, Tsolaki AG, Yasmin H, Klein L, Singh SK, Kishore U (2020) Molecular Heterogeneity and Immunosuppressive Microenvironment in Glioblastoma. *Front Immunol* 11:1402. <https://doi.org/10.3389/fimmu.2020.01402>
42. Bastid J, Regairaz A, Bonnefoy N, Dejou C, Giustiniani J, Laheurte C, Cochaud S, Laprevotte E, Funck-Bretano E, Hemon P, Gros L, Bec N, Larroque C, Alberici G, Bensussan A, Eliaou JF (2015) Inhibition of CD39 enzymatic function at the surface of tumor cells alleviates their immunosuppressive activity. *Cancer Immunol Res* 3(3):254–265. <https://doi.org/10.1158/2326-6066.CIR-14-0018>
43. Di Virgilio F, Falzoni S, Giuliani AL, Adinolfi E (2016) P2 receptors in cancer progression and metastatic spreading. *Curr Opin Pharmacol* 29:17–25. <https://doi.org/10.1016/j.coph.2016.05.001>
44. Coy S, Wang S, Stopka SA, Lin JR, Yapp C, Ritch CC, Salhi L, Baker GJ, Rashid R, Baquer G, Regan M, Khadka P, Cole KA, Hwang J, Wen PY, Bandopadhyay P, Santi M, Raedt TD, Ligon KL, Agar NYR, Sorger PK, Touat M, Santagata S (2022) Single cell spatial analysis reveals the topology of immunomodulatory purinergic signaling in glioblastoma. *Nat Commun* 13(1):4814. <https://doi.org/10.1038/s41467-022-32430-w>
45. Seager RJ, Hajal C, Spill F, Kamm RD, Zaman MH (2017) Dynamic interplay between tumour, stroma and immune system can drive or prevent tumour progression. *Converg Sci Phys Oncol* 3. <https://doi.org/10.1088/2057-1739/aa7e86>
46. Ungefroren H, Sebens S, Seidl D, Lehnert H, Hass R (2011) Interaction of tumor cells with the microenvironment. *Cell Commun Signal* 9(18). <https://doi.org/10.1186/1478-811X-9-18>
47. Azambuja JH, Ludwig N, Yerneni S, Rao A, Braganhol E, Whiteside TL (2020) Molecular profiles and immunomodulatory activities of glioblastoma-derived exosomes. *Neuro-Oncology Adv*. <https://doi.org/10.1093/nojnl/vdaa056>
48. Deaglio S, Dwyer KM, Gao W, Friedman D, Usheva A, Erat A, Chen JF, Enjyoji K, Linden J, Oukka M, Kuchroo VK, Strom TB, Robson SC (2007) Adenosine generation catalyzed by CD39 and CD73 expressed on regulatory T cells mediates immune suppression. *J Exp Med* 204(6):1257–1265. <https://doi.org/10.1084/jem.20062512>
49. Desland FA, Hormigo A (2020) The CNS and the Brain Tumor Microenvironment: Implications for Glioblastoma Immunotherapy. *Int J Mol Sci* 21(19). <https://doi.org/10.3390/ijms21197358>
50. Sampson JH, Gunn MD, Fecci PE, Ashley DM (2020) Brain immunology and immunotherapy in brain tumours. *Nat Rev Cancer* 20(1):12–25. <https://doi.org/10.1038/s41568-019-0224-7>
51. Mandapathil M, Lang S, Gorelik E, Whiteside TL (2009) Isolation of functional human regulatory T cells (Treg) from the peripheral blood based on the CD39 expression. *J Immunol Methods* 346:55–63. <https://doi.org/10.1016/j.jim.2009.05.004>
52. Takenaka MC, Robson SC, Quintana FJ (2016) Regulation of the T Cell Response by CD39. *Trends Immunol* 37(7):427–439. <https://doi.org/10.1016/j.it.2016.04.009>
53. Heimberger AB, Abou-Ghazal M, Reina-Ortiz C, Yang DS, Sun W, Qiao W, Hiraoka N, Fuller GN (2008) Incidence and prognostic impact of FoxP3+ regulatory T cells in human gliomas. *Clin Cancer Res* 14(16):5166–5172. <https://doi.org/10.1158/1078-0432.CCR-08-0320>
54. Sayour EJ, McLendon P, McLendon R, De Leon G, Reynolds R, Kresak J, Sampson JH, Mitchell DA (2015) Increased proportion of FoxP3+ regulatory T cells in tumor infiltrating lymphocytes is associated with tumor recurrence and reduced survival in patients with glioblastoma. *Cancer Immunol Immunother* 64(4):419–427. <https://doi.org/10.1007/s00262-014-1651-7>
55. Vivier E, Ugolini S (2015) Regulatory natural killer cells: new players in the IL-10 anti-inflammatory response. *Cell Host Microbe* 6(6):493–495. <https://doi.org/10.1016/j.chom.2009.12.001>
56. Yang R, Cheng S, Luo N, Gao R, Yo K, Kang B, Wang L, Zhang Q, Fang Q, Zhang L, Li C, He A, Hu X, Peng J, Ren X, Zhang Z (2019) Distinct epigenetic features of tumor-reactive CD8+



- T cells in colorectal cancer patients revealed by genome-wide DNA methylation analysis. *Genome Biol* 21(1):2. <https://doi.org/10.1186/s13059-019-1921-y>
57. Qi Y, Xia Y, Lin Z, Qi Y, Chen Y, Zhou Q, Zhen H, Wang J, Chang Y, Bai Q, Wang Y, Zhu Y, Xu L, Chen L, Kong Y, Zhang W, Dai B, Liu L, Guo J, Xu J (2020) Tumor-infiltrating CD39(+)/CD8(+) T cells determine poor prognosis and immune evasion in clear cell renal cell carcinoma patients. *Cancer Immunol Immunother* 69(8):1565–1576. <https://doi.org/10.1007/s00262-020-02563-2>
  58. Simoni Y et al (2018) Bystander CD8(+) T cells are abundant and phenotypically distinct in human tumour infiltrates. *Nature* 557(7706):575–579. <https://doi.org/10.1038/s41586-018-0130-2>
  59. Soares A, Govender L, Hughes J, Mavakla W, Kock M, Bernard C, Pienaar B, Rensburg EJ, Jacobs G, Khomba G, Stone L, Abel B, Scriba TJ, Hanekon WA (2010) Novel application of Ki67 to quantify antigen-specific in vitro lymphoproliferation. *J Immunol Methods* 362(1):43–50. <https://doi.org/10.1016/j.jim.2010.08.007>
  60. Baitsch L, Baumgaertner P, Devevre E, Raghav SK, Legat A, Barba L, Wieckowski S, Bouzourene H, Deplancke B, Romero P, Rufer N, Speiser DE (2011) Exhaustion of tumor-specific CD8<sup>+</sup> T cells in metastases from melanoma patients. *J Clin Invest* 121(6):2350–2360. <https://doi.org/10.1172/JCI46102>
  61. Duhon T, Duhon R, Montler R, Moses J, Moudgil T, Miranda NF, Goodall CP, Blair TC, Fox BA, McDermott JE, Chang SC, Grunkemeier G, Leidner R, Bell RB, Weinberg AD (2018) Co-expression of CD39 and CD103 identifies tumor-reactive CD8 T cells in human solid tumors. *Nat Commun* 9(1):2724. <https://doi.org/10.1038/s41467-018-05072-0>
  62. Workel HH, Rooji NV, Plat A, Spierings DCJ, Fehrmann RSN, Nijman HW, Bruyn M (2020) Transcriptional Activity and Stability of CD39+CD103+CD8+ T Cells in Human High-Grade Endometrial Cancer. *Int J Mol Sci* 21(11). <https://doi.org/10.3390/ijms21113770>
  63. Liu T, Tan J, Wu M, Fan W, Wei J, Zhu B, Guo J, Wang S, Zhou P, Zhang H, Shi L, Li J (2021) High-affinity neoantigens correlate with better prognosis and trigger potent antihepatocellular carcinoma (HCC) activity by activating CD39+CD8+ T cells. *Gut* 70(10):1965. <https://doi.org/10.1136/gutjnl-2020-322196>
  64. DiLillo DJ, Yanaba K, Tedder TF (2010) B cells are required for optimal CD4+ and CD8+ T cell tumor immunity: therapeutic B cell depletion enhances B16 melanoma growth in mice. *J Immunol* 184(7):4006–4016. <https://doi.org/10.4049/jimmunol.0903009>
  65. Burger JA, Wiestner A (2018) Targeting B cell receptor signaling in cancer: preclinical and clinical advances. *Nat Rev Cancer* 18(3):148–167. <https://doi.org/10.1038/nrc.2017.121>
  66. Saze Z, Schuler P, Hong C, Cheng D (2013) Adenosine production by human B cells and B cell-mediated suppression of activated T cells. *Blood* 122:9–19. <https://doi.org/10.1182/blood-2013-02-482406.Z.S>
  67. Quarona V, Zaccarello G, Chillemi A, Brunetti E, Singh VK, Ferrero E, Funaro A, Horenstein AL, Malavasi F (2013) CD38 and CD157: a long journey from activation markers to multifunctional molecules. *Cytometry B Clin Cytom* 84(4):207–217. <https://doi.org/10.1002/cyto.b.21092>
  68. Bahri R, Bollinger A, Bollinger T, Orinska Z, Bulfone-Paus S (2012) Ectonucleotidase CD38 demarcates regulatory, memory-like CD8+ T cells with IFN- $\gamma$ -mediated suppressor activities. *PLoS One* 7(9):e45234. <https://doi.org/10.1371/journal.pone.0045234>
  69. Chen L et al (2018) CD38-Mediated Immunosuppression as a Mechanism of Tumor Cell Escape from PD-1/PD-L1 Blockade. *Cancer Discov* 8(9):1156–1175. <https://doi.org/10.1158/2159-8290.CD-17-1033>
  70. Rosser EC, Mauri C (2015) Regulatory B Cells: Origin, Phenotype, and Function. *Immunity* 42(4):607–612. <https://doi.org/10.1016/j.immuni.2015.04.005>
  71. Chen PY, Wu CYJ, Fang JH, Chen HC, Feng LY, Huang CY, Wei KC, Fang JY, Lin CY (2019) Functional Change of Effector Tumor-Infiltrating CCR5(+)/CD38(+)/HLA-DR(+)/CD8(+) T Cells in Glioma Microenvironment. *Front Immunol* 10:2395. <https://doi.org/10.3389/fimmu.2019.02395>
  72. Flores-Borja F, Bosma A, Ng D, Reddy V, Ehrenstein MR, Isenberg DA, Mauri C (2013) CD19+CD24hiCD38hi B cells maintain regulatory T cells while limiting TH1 and TH17 differentiation. *Sci Transl Med* 5(173):173ra23. <https://doi.org/10.1126/scitranslmed.3005407>
  73. Wang WW, Yuan XL, Chen H, Xie GH, Ma YH, Zheng YX, Zhou YL, Shen LS (2015) CD19+CD24hiCD38hi Bregs involved in downregulate helper T cells and upregulate regulatory T cells in gastric cancer. *Oncotarget* 6(32):33486–33499. <https://doi.org/10.18632/oncotarget.5588>
  74. Patton DT, Wilson MD, Rowan WC, Soond DR, Okkenhaug K (2011) The PI3K p110 $\delta$  regulates expression of CD38 on regulatory T cells. *PLoS One* 6(3):e17359. <https://doi.org/10.1371/journal.pone.0017359>
  75. Feng X, Zhang L, Acharya C, An G, Wen K, Qiu L, Munshi NC, Tai YT, Anderson KC (2017) Targeting CD38 Suppresses Induction and Function of T Regulatory Cells to Mitigate Immunosuppression in Multiple Myeloma. *Clin Cancer Res* 23(15):4290–4300. <https://doi.org/10.1158/1078-0432.CCR-16-3192>
  76. Tang Z, Li C, Kang B, Gao G, Li C, Zhang Z (2017) GEPIA: a web server for cancer and normal gene expression profiling and interactive analyses. *Nucleic Acids Res* 45:W98–W102. <https://doi.org/10.1093/nar/gkx247>
  77. Perenkov AD, Novikov DV, Sakharnov NA, Aliasova AV, Utkin OV, Baryshnikov AI, Novikov VV (2012) Heterogeneous expression of CD38 gene in tumor tissue in patients with colorectal cancer. *Mol Biol (Mosk)* 46(5):786–791
  78. Chmielewski JP, Bowlby SC, Wheeler FB, Shi L, Sui G, Davis AL, Howard TD, D'Agostino RB, Miller LD, Sirintrapun SJ, Cramer SD, Kridel SJ (2020) CD38 Inhibits Prostate Cancer Metabolism and Proliferation by Reducing Cellular NAD(+) Pools. *Mol Cancer Res* 16(11):1687–1700. <https://doi.org/10.1158/1541-7786.MCR-17-0526>
  79. Zhu Y, Zhang Z, Jiang Z, Liu, Y, Zhou J (2020) CD38 Predicts Favorable Prognosis by Enhancing Immune Infiltration and Antitumor Immunity in the Epithelial Ovarian Cancer Microenvironment. *Front Genet* 11. <https://doi.org/10.3389/fgene.2020.00369>
  80. Rockenbach L, Braganhol E, Dietrich F, Figueiro F, Pugliesi M, Edelweiss MI, Morrone FB, Sévigny J, Battastini AMO (2014) NTPDase3 and ecto-5'-nucleotidase/CD73 are differentially expressed during mouse bladder cancer progression. *Purinergic Signal* 10(3):421–430. <https://doi.org/10.1007/s11302-014-9405-8>
  81. Yu W, Robson SC, Hill WG (2011) Expression and distribution of ectonucleotidases in mouse urinary bladder. *PLoS One* 6(4):e18704. <https://doi.org/10.1371/journal.pone.0018704>
  82. Huang J, Chen MN, Du J, Liu H, He YJ, Li GL, Li SY, Liu WP, Long XY (2016) Differential Expression of Adenosine P1 Receptor ADORA1 and ADORA2A Associated with Glioma Development and Tumor-Associated Epilepsy. *Neurochem Res* 41(7):1774–1783. <https://doi.org/10.1007/s11064-016-1893-1>
  83. Bauer A, Langen KJ, Bidmon H, Holschbach MH, Weber S, Olsson RA, Coenen HH, Zilles K (2005) m18F-CPFPX PET identifies changes in cerebral A1 adenosine receptor density caused by glioma invasion. *J Nucl Med* 46(3):450–454
  84. Takenaka MC, Gabriely G, Rothhammer V, Mascanfroni ID, Wheeler MA, Chao CC, Gutierrez-Vazquez C, Kenison J, Tjon

- EC, Barroso A, Vandeventer T, Lima KA, Rothweiler S, Mayo L, Ghannan S, Zandee S, Healy L, Sherr D, Farez MF, Prat A, Antel J, Reardon DA, Zhang H, Robson SC, Quintana FJ (2019) Control of tumor-associated macrophages and T cells in glioblastoma via AHR and CD39. *Nat Neurosci* 22(5):729–740. <https://doi.org/10.1038/s41593-019-0370-y>
85. Yan A, Joachims ML, Thompson LF, Miller AD, Canoll PD, Bynoe MS (2019) CD73 Promotes Glioblastoma Pathogenesis and Enhances Its Chemoresistance via A(2B) Adenosine Receptor Signaling. *J Neurosci Off J Soc Neurosci* 39(22):4387–4402. <https://doi.org/10.1523/JNEUROSCI.1118-18.2019>
86. Bova V, Filippone A, Casili G, Lanza M, Compolo M, Capra AP, Repici A, Crupi L, Motta G, Colorossi C, Chisari G, Cuzzocrea S, Esposito E, Paterniti I (2022) Adenosine Targeting as a New Strategy to Decrease Glioblastoma Aggressiveness. *Cancers (Basel)* 14(16). <https://doi.org/10.3390/cancers14164032>
87. Kitabatake K, Kaji T, Tsukimoto M (2021) Involvement of CD73 and A2B Receptor in Radiation-Induced DNA Damage Response and Cell Migration in Human Glioblastoma A172 Cells. *Biol Pharm Bull* 44(2):197–210. <https://doi.org/10.1248/bpb.b20-00654>
88. Ott M, Tomaszowski KH, Marisetty A, Kong LY, Wei J, Duna M, Blumberg K, Ji X, Jacobs C, Fuller GN, Langford LA, Huse JT, Long JP, Hu J, Li S, Weinberg JS, Prabhu SS, Sawaya R, Ferguson S, Rao G, Lang FF, Curran MA, Heimberger AB (2020) Profiling of patients with glioma reveals the dominant immunosuppressive axis is refractory to immune function restoration. *JCI insight* 5(17). <https://doi.org/10.1172/jci.insight.134386>
89. Kohanbash G, Carrera DA, Shrivastav S, Ahn BJ, Jahan N, Mazor T, Chheda ZS, Downey KM, Watchmaker PB, Beppler C, Warta R, Amankulor NA, Herold-Mende C, Costello JF, Okada H (2017) Isocitrate dehydrogenase mutations suppress STAT1 and CD8+ T cell accumulation in gliomas. *J Clin Invest* 127(4):425–437. <https://doi.org/10.1172/JCI90644>
90. Notarangelo G et al (2022) Oncometabolite d-2HG alters T cell metabolism to impair CD8(+) T cell function. *Science* 377(6614):1519–1529. <https://doi.org/10.1126/science.abj5104>

**Publisher's Note** Springer Nature remains neutral with regard to jurisdictional claims in published maps and institutional affiliations.

Springer Nature or its licensor (e.g. a society or other partner) holds exclusive rights to this article under a publishing agreement with the author(s) or other rightsholder(s); author self-archiving of the accepted manuscript version of this article is solely governed by the terms of such publishing agreement and applicable law.